New boron isotopic evidence for sedimentary and magmatic fluid influence in the shallow hydrothermal vent system of Milos Island (Aegean Sea, Greece)

Wu, Shein-fu; You, Chen-feng; Lin, Yen-po; Valsami-jones, Eugenia; Baltatzis, Emmanuel

DOI:
10.1016/j.jvolgeores.2015.11.013

Document Version
Peer reviewed version

Citation for published version (Harvard):
Wu, S, You, C, Lin, Y, Valsami-jones, E & Baltatzis, E 2016, 'New boron isotopic evidence for sedimentary and magmatic fluid influence in the shallow hydrothermal vent system of Milos Island (Aegean Sea, Greece)', *Journal of Volcanology and Geothermal Research*, vol. 310, pp. 58-71. https://doi.org/10.1016/j.jvolgeores.2015.11.013

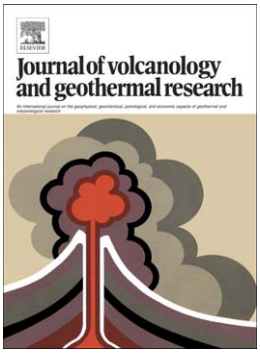

New Boron Isotopic Evidence for Sedimentary and Magmatic Fluid Influence in the Shallow Hydrothermal Vent System of Milos Island (Aegean Sea, Greece)

Shein-Fu Wu, Chen-Feng You, Yen-Po Lin, Eugenia Valsami-Jones, Emmanuel Baltatzis

PII: S0377-0273(15)00387-X
DOI: doi: 10.1016/j.jvolgeores.2015.11.013
Reference: VOLGEO 5707

To appear in: *Journal of Volcanology and Geothermal Research*

Received date: 22 April 2015
Accepted date: 14 November 2015

Please cite this article as: Wu, Shein-Fu, You, Chen-Feng, Lin, Yen-Po, Valsami-Jones, Eugenia, Baltatzis, Emmanuel, New Boron Isotopic Evidence for Sedimentary and Magmatic Fluid Influence in the Shallow Hydrothermal Vent System of Milos Island (Aegean Sea, Greece), *Journal of Volcanology and Geothermal Research* (2015), doi: 10.1016/j.jvolgeores.2015.11.013

New Boron Isotopic Evidence for Sedimentary and Magmatic Fluid Influence in the Shallow Hydrothermal Vent System of Milos Island (Aegean Sea, Greece)

Shein-Fu Wu[1, 2], Chen-Feng You[1]*, Yen-Po Lin[1], Eugenia Valsami-Jones[3], Emmanuel Baltatzis[4]

[1] Department of Earth Sciences, National Cheng-Kung University, No. 1 University Rd., Tainan 701, Taiwan

also at Earth Dynamic System Research Center, NCKU, Tainan 701, Taiwan

[2] Institute of Oceanography, National Taiwan University, No. 1, Sec. 4, Roosevelt Road, Taipei 106, Taiwan

[3] School of Geography, Earth and Environmental Sciences, University of Birmingham, B15 2TT, UK

[4] Department of Geology and Geoenvironment, National and Kapodistrian University of Athens, Athens, GR 157 84, Greece

Corresponding author:

Chen-Feng You

E-mail address: cfy20@mail.ncku.edu.tw

Tel: 886-6-2757575 ext.65438

Shein-Fu Wu

E-mail address: sheinfuwu@ntu.edu.tw

Tel: 886-2-23636040 ext.111

Abstract

Magmatic sources may contribute a significant amount of volatiles in geothermal springs; however, their role is poorly understood in submarine hydrothermal systems worldwide. In this study, new results of B and $\delta^{11}B$ in 41 hydrothermal vent waters collected from the shallow hydrothermal system of Milos island in the Aegean Sea were combined with previously published data from other tectonic settings and laboratory experiments to quantify the effects of phase separation, fluid/sediment interaction and magmatic contribution. Two Cl-extreme solutions were identified, high-Cl waters (Cl as high as 2000 mM) and low-Cl waters (Cl <80 mM). Both sets of waters were characterized by high B/Cl (~1.2–5.3×10^{-3} mole/mole) and extremely low $\delta^{11}B$ (1.4–6.3‰), except for the waters with Mg content of near the seawater value and $\delta^{11}B$=10.3-17.4‰. These high-Cl waters with high B/Cl and low $\delta^{11}B$ plot close to the vent waters in sediment-hosted hydrothermal system (i.e., Okinawa Trough) or fumarole condensates from on-land volcanoes, implying B addition from sediment or magmatic fluids plays an important role. This is in agreement with fluid/sediment interactions resulting in the observed B and $\delta^{11}B$, as well as previously reported Br/I/Cl ratios, supporting a scenario of slab-derived fluid addition with elevated B, ^{11}B-rich, and low Br/Cl and I/Cl, which is derived from the dehydration of subducted-sediments. The slab fluid becomes subsequently mixed with the parent magma of Milos. The deep brine reservoir is partially affected by injections of magmatic fluid/gases during degassing. The results presented here are crucial for deciphering the evolution of the brine reservoirs involved in phase separation, fluid/sediment interaction and magmatic contribution in the deep reaction zone of the Milos hydrothermal system; they also have implications in the understanding of the formation of metallic vein mineralization.

Key words: hydrothermal system, boron isotope, water/rock interaction, magmatic fluids, Milos

1. Introduction

Many hydrothermal systems have been discovered in tectonic settings ranging from sediment-starved mid-ocean ridge (MOR) and back-arc basin (BAB), to sediment-hosted ridges (SR)(Butterfield et al., 1990; Campbell and Edmond, 1989; Campbell et al., 1988; Fouquet et al., 1991; Lonsdale, 1977; Von Damm and Bischoff, 1987; Von Damm et al., 1985a, 1985b). The fluids discharging from the hydrothermal vents found in such systems can play critical role in the chemical mass balance of ocean. Moreover, the fluids influence profoundly the chemistry of the surrounding rocks in the discharge zones, with significant physicochemical transformations occurring in shallow hydrothermal vents compared with the deep-sea environments (Botz et al., 1996; Fitzsimons et al., 1997; Ishibashi et al., 2008; McCarthy et al., 2005; Pichler et al., 1999; Prol-Ledesma et al., 2004; Tassi et al., 2009). However, a systematic comparison of fluid chemistry in terms of the degree of fluid-rock/sediment interaction and the effects of phase separation among MOR, BAB, SR, and shallow-water systems has not been carried out. Magmatic heating provides common driving forces for hydrothermal circulation at mid-ocean ridges and on-land volcanoes. Occurrences of noble and volatile gases, as well as elemental and isotopic changes in chemistry, have been documented in detail, after magmatic intrusion or volcanic eruptions. These results emphasize the importance of magmatic inputs in hydrothermal fluids (Ruzié et al., 2012; Seyfried et al., 2003; Somoza et al., 2004; Urabe et al., 1995; Von Damm, 2000; Von Damm et al., 2003). Several studies have suggested variable pathways of magmatic gas/water evolution to cause widespread chemical compositional variation in shallow-water systems, making them good analogues for systems occurring in mid-ocean ridges or on land (Capaccioni et al., 2005; 2007; Tassi et al., 2009; Sedwick and Stüben, 1996). However, the role of magmatic inputs at shallow-sea hydrothermal system remains poorly constrained.

Boron has two stable isotopes, ^{10}B and ^{11}B, with natural abundances of 19.9 and 80.1

%, respectively. In seawater, B is present as boric acid ($B(OH)_3$, a trigonal species) and borate ions ($B(OH)_4^-$, a tetrahedral species). The ion exchange reaction of ^{10}B and ^{11}B between the two species is described as:

$$^{11}B(OH)_3 + ^{10}B(OH)_4^- = ^{10}B(OH)_3 + ^{11}B(OH)_4^-.$$

Previously experimental data indicated that $B(OH)_3$ is enriched in ^{11}B relative to $B(OH)_4^-$ (Kakihana et al., 1977; Klochko et al., 2006). Their relative proportions are generally a function of pH where the predominant isotopic fractionation occurs via equilibrium exchange between the two aqueous species, $B(OH)_3$ dominates at low pH and $B(OH)_4^-$ at high pH (Hershey et al., 1986; Kakihana et al., 1977; ; Spivack and Edmond, 1987). Boron isotopes provide useful information for deciphering the origins and evolution mechanisms of vent fluids in various geological settings due to the large relative mass difference between the two isotopes and their high geochemical reactivity, which caused significant B isotopic fractionations (e.g., Palmer, 1991; Palmer and Sturchio, 1990; Spivack and Edmond, 1987; Spivack et al., 1987; You et al., 1993, 1994). Almost linear co-variation of B/Cl with 1/Cl is evident in laboratory liquid-vapor phase separation experiments. The observed small difference in B/Cl and 1/Cl trends between experiments and field data indicates that phase separation predominantly controls the Cl concentration in both phases in MOR system (Berndt and Seyfried, 1990; Bischoff and Rosenbauer, 1987; You et al., 1994). B isotopic fractionation is associated with boiling and phase separation in thermal waters, whereby ^{11}B partitions selectively into the vapor phase (Liebscher et al., 2005; Leeman et al., 1992; Spivack et al., 1990). However, empirical and experimental data indicate that B isotopic difference between liquid and vapor is rather small (–3 to –1‰ at ~140–300 °C) and decreases with increasing temperature, with negligible isotopic fractionation above 400 °C (Liebscher et al., 2005; Palmer and Sturchio, 1990; Spivack et al., 1990). The B enrichment in oceanic rocks induced by seafloor alteration, mainly relates to low-temperature

mineralogical changes, such as substitution of primary minerals by smectite and palagonitization of basaltic glass during seawater percolation (Seyfried et al., 1984; Spivack and Edmond, 1987). The B and $\delta^{11}B$ in different geochemical reservoirs showed extremely wide distribution, ranging from < 0.1 to >100 ppm and –30 to +60‰ (relative to the NBS SRM-951), respectively (Barth, 1993; Bebout et al., 1993). The dissolved B in these reservoir fluids often represents mixtures of different origins: natural hydrothermal fluids and altered rocks/sediments (Berndt and Seyfried, 1990; Palmer, 1991; Spivack and Edmond, 1987; You et al., 1994). There are several previous studies of B and B isotopic composition in fumarolic condensates and geothermal fluids from volcanic regions (e.g. Vulcano Island, Italy; Taupo volcanic zone, New Zealand); in those studies, the distinct end-member fluid composition for reconstruction of temporal evolution of magmatic sources was identified (Leeman et al., 2005; Millot et al., 2012; Reyes and Trompetter, 2012). In addition, high B/Cl ratio in discharging fluids was ascribed to input of B-enriched component and was used as a proxy for CO_2/Cl to trace the magmatic addition (Giggenbach, 1995).

Based on stable isotope data, specifically S isotope and noble gases data, previous efforts have emphasized the importance of seawater and magmatic water components at the island of Milos, as well as the islands of Santorini and Nisyros, and perhaps in the whole Aegean volcanic arc, although the magmatic contribution is still ambiguously argued (Botz et al., 1996; Brombach et al., 2003; Dotsika et al., 2009; Marini et al., 2002; Naden et al., 2005; Price et al., 2013; Shimizu et al., 2005). A time-series study of fluid chemistry could provide a more clear view that would enable a better understanding of the processes on Milos. In this study, 41 new samples of vent fluids from a 2003 expedition on Milos were analyzed for B and $\delta^{11}B$, bringing a new perspective in the understanding of candidates of source fluids in the hydrothermal system. The data are complemented by a compilation of other published geochemical results of fluids or fumarolic condensates from Milos and other locations in the

Aegean geothermal system, as well as various other submarine hydrothermal systems (e.g., MOR, BAB, SR) and subaerial volcanoes (e.g., Taupo volcano, New Zealand; Vulcano Island, Italy). We aim to utilize new and published results of B, $\delta^{11}B$, B/Cl and literature data of halogen (Cl, Br, I) to examine the sources and evolutionary history of the deep saline reservoir, as well as to elucidate the role of vapor-brine phase separation, magmatic fluids, and fluid/sediment interaction in the Milos system.

2. Samples and experiments

2.1 Geological settings

The subduction of the African plate beneath the Eurasian plate has resulted in the formation of the Mediterranean Ridge and the Hellenic Trench, as well as volcanism in the Aegean volcanic arc and the back-arc extension in the Aegean Sea (Agostini et al., 2010; McKenzie, 1970, 1972; Ring et al., 2010). The Aegean volcanic arc is constituted from west to east by the islands of Methana, Milos, Santorini, Kos and Nisyros (Fig. 1) (e.g. Shimizu et al., 2005; Varnavas and Cronan, 2005). The islands of the central-eastern part of the arc (Milos, Santorini, and Nisyros) are presently active geothermal systems, while Methana and Kos display declining hydrothermal activity (Dotsika et al., 2009; Shimizu et al., 2005). The volcanic rocks compositions of arc islands are associated with calc-alkaline and high-K calc-alkaline exception of basalts presented in Santorini island group (Francalanci et al., 2005). The age determinations of erupted lava suggested that the islands lying on the south of volcanic arc (e.g. Methana, Milos, Santorini and Nisyros) show younger ages relative to those from the islands on the north side of arc (e.g. Aegina, Kos), implying the southward migration of volcanic front (Francalanci et al., 2005; Matsuda et al., 1999). Papazachos et al (1995) reported that the continental crust is relatively thinner in the central sector of the arc than the western and eastern sectors, constraining the influence of shallow crustal

contamination effect for magma genesis. The volcanism on Milos Island started from 3.5 to 0.08 Ma, subsequently the volcanic sequence was overlain by recent alluvial deposits (Fytikas, 1989; Fytikas et al., 1986). Several main cycles of volcanic activity have been distinguished, including the initial submarine eruptions and the followed pyroclastic material deposition, which resulted from subaerial eruptions that composed mainly of lava domes and flows (Fytikas et al., 1986). This island is mostly composed of calc-alkaline series volcanic rocks, which range from basaltic andesites to dacites, and rhyolites (Fytikas, 1989; Fytikas et al., 1986). The bulk sediment inshore shows a dominant detrital fraction and is highly influenced by hydrothermal activity (Varnavas and Cronan, 2005).

2.2 Sample location, collection and analytical methods

There are abundant discharges of hot water and steam distributed either on land or offshore within shallow depth at Milos. CO_2 (as high of ~90% v/v) is the dominant component of gas venting (Botz et al., 1996; Dando et al., 1995). Various types of fluid discharge are surrounding the coast of Milos, including intense degassing with steams, emenating of saline fluid as brine pool and diffusive warm fluid (Price et al., 2013; Valsami-Jones et al., 2005). Wells drilled in past years in the Zephyria area as part of the geothermal exploration of the island, reached a maximum depth of 1101–1381 m and found evidence for a saline reservoir distributed at depth 1–2 km with chlorinity of > 2.5 times seawater value and temperature of 300–325 °C (Fig. 1)(Dotsika et al., 2009; Fitzsimons et al., 1997; Liakopoulos et al., 1991). There are at least two recoganised types of hydrothermal waters on the island: low chlorinity fluids (discharging subaerially in a cave and in a number of shallow submarine locations) and high chlorinity fluid discharging underwater (Valsami-Jones et al., 2005). All samples, except from the low-Cl cave fluid, were sampled from shallow (up to 10 m depth) underwater vents from the location of the main activity on

the island, Palaeohori Bay where the most intense hydrothermal activities were reported (Fig. 1). These locations were sampled during two expeditions in the years 2002 and 2003. There are two neighboring on-shore springs with significantly low salinity and pH discharging through rock fissures immediately above the sea level (Cave #1 and #2); these were monitored over several years (Fig. 1)(Valsami-Jones et al., 2005; Wu et al., 2011, 2012). Ambient seawaters away from any hydrothermal influences were also collected for reference.

In-situ temperatures of venting samples were measured using a "HANNA" (HI 9063) thermal meter at the focused venting sites. After at least three rinses, venting fluid was collected using a 50 cm^3 plastic bottles, previously cleaned with distilled nitric acid; the samples were taken as close as possible to the hottest point of discharge to minimize contamination by ambient seawater. Subsequently the fluid was filtered into a clean bottle using a 0.2 μm cellulose acetate filter. After collection, the bottles were sealed tightly and transported back to the laboratory for further chemical and isotopic analyses. The pH of vent fluid was determined separately at ambient temperature after allowing the sample to cool in a covered bottle.

These vent samples including ambient seawaters, were treated with 150–1000-fold dilution depending on chlorinity variation by sub-boiling 0.3M HNO_3 for elemental determination using ICP-MS (Thermo Scientific MAT Element 2) in the Isotope Geochemistry Laboratory (IGL) at the National Cheng-Kung University, Taiwan. The standard seawaters used for method testing included IAPSO and NASS-5 and were separately prepared as a series of matrix calibration solutions for major and trace element determination. Major element (e.g., Na, Cl, K, Mg, and Ca) and B measurements were carried out using low, medium, and high resolution modes to prevent interferences. Procedure blanks were monitored every five analyses and the IAPSO standard solution was determined every 10 measurements to monitor instrumental stability and drift. The obtained average analytical

precision for major and minor elements were reported as better than 3% (RSD) (Wu et al., 2011; 2012). The average analytical precision of B concentrations in 2003 vent samples is 2.69% (RSD) in this study. The concentration of SO_4 in vent samples during two expeditions was determined by ion chromatography (IC).

For the isotopic B composition determination, micro-sublimation purification procedures were adopted to ensure that none of the samples had any mass loss during sublimation procedures and to reduce matrix effects from salt and/or organics (Gaillardet et al., 2001; Wang et al., 2010). A droplet of sample fluid containing volatile B (50 ng) was carefully separated into a supernatant solution after heating at 98 °C for 12 hours and subsequently diluted by sub-boiling HNO_3 for further isotopic B composition measurements using MC-ICP-MS with standard-sample bracketing procedure (Thermo Scientific Neptune at EDSRC, National Cheng-Kung University, Taiwan). The detailed evaluation of MC-ICP-MS analysis coupled with B micro-sublimation were reported by Wang et al. (2010). The B isotope ratio is expressed as δ^{11}B-values relative to NBS SRM-951 standard, and is described as:

$$\delta^{11}B\ (‰) = [(^{11}B/^{10}B)_{sample}/(^{11}B/^{10}B)_{standard} - 1]*10^3$$

where the standard is NBS boric acid SRM-951. The long-term external precision from repeated analyses of 20 and 50 ppb NBS 951 standard is separately of 0.26‰ (2SD, n = 5) and 0.25‰ (2SD, n = 4) in our laboratory.

The end-member (EM) composition of hydrothermal fluid at each sampling site was calculated based on the near-zero Mg assumption in fluid-seawater mixing trend, following a linear regression between pure hydrothermal fluid (zero Mg content) and seawater (see Fig. 2)(Bischoff and Dickson, 1975). Similarly, Mg content was normalized to B content for its isotopic evaluation, the EM δ^{11}B is defined from the linear mixing correlation (see Fig. 2f) (Hinkley and Tatsumoto, 1987).

2.3 Simulation of fluid-rock interaction

The degree of water/rock interaction critically regulates the EM chemical compositions in hydrothermal waters during seawater percolation in hydrothermal systems and leads to major ion enrichment in reservoir liquids (e.g., Bischoff and Rosenbauer, 1984; Bischoff and Dickson, 1975; Seyfried, 1987; Seyfried and Bischoff, 1979). The effect of fluid-rock interaction may be simulated using an approach developed by Banner and Hanson (1990). The elemental B concentration (C_0) in a system prior to interaction with an initial (unreacted) percolated fluid into a given volume of rock with known porosity may be given by mass balance as below:

$$C_0=F\times C_{f,0}+(1-F)\times C_{r,0} \quad (1)$$

where F and (1-F) are the weight fraction of fluid and rock separately in the system for any iteration; $C_{f,0}$ and $C_{r,0}$ are B concentrations in fluid and solid rock, respectively, before interaction. F is related to porosity using densities in fluid and rock by,

$$F=(P\times\rho_f)/(P\times\rho_f+(1-P)\rho_r) \quad (2)$$

P represents the porosity in volume fraction and ρ_f, ρ_r are the densities of the fluid and solid rock, respectively. The composition of fluid and rock after equilibration can be determined using distribution coefficient $D_{r\text{-}f}$ to calculate the elemental B concentration in the fluid (C_f) equilibrated with rock:

$$C_f= C_r/(D_{r\text{-}f}) \quad (3)$$

Combining the Eqn. (1) and (3), we can solve for C_r, which is the equilibrated B concentration in rock,

$$C_r= C_0/[F/(D_{r\text{-}f})+(1-F)] \quad (4)$$

We consider the calculation in open-system fluid-rock interaction to simulate the progressive changes of the composition of rock upon repeated additions of fluid with same initial composition, and the reacted fluid being displaced by the introduction of unreacted

fluid after each iteration. It is assumed that percolated seawater transported through the fractures of rock can be determined by iterative calculation, combining firstly the Eqn. (1) and (4) to solve the equilibrated composition of rock, C_r. Then, the calculated C_r from Eqn. (4) is taken to represent B concentration in rock ($C_{r,0}$) for the next iteration of Eqn. (1). In this simulation, we simply assumed a constant porosity of 20%, because porosity is poorly known and may differ in a varied geological setting such as that of Milos. The cumulative fluid-rock ratio (w/r ratio) for any stage in the interaction process is expressed on a weight basis, as the term of N,

$$N=n\times(F/(1-F)) \qquad (5)$$

where n is the number of iteration, and F/(1-F) is the incremental fluid-rock ratio.

The isotopic composition of fluid and rock upon equilibration during interaction depends on the isotopic composition of the total system, the fractionation factor between rock and fluid, and the proportion of both phases in system. The mass balance calculation of isotopic B value of total fluid-rock system for each iteration is described as follows:

$$\delta^{11B}_0=[(\delta^{11B}_{f,0})*(C_{f,0})*F+(\delta^{11B}_{r,0})*(C_{r,0})*(1-F)]/C_0 \qquad (6)$$

where C_0 is calculated in Eqn. (1) and is constant for given F. For the first iteration, δ^{11B}_0 is the isotopic composition for the entire system and is obtained by Eqn. (6) for given initial end-component values of $\delta^{11B}_{f,0}$ and $\delta^{11B}_{r,0}$ in seawater and rock, respectively.

After equilibration, $\delta^{11B}_{f,0}$ and $\delta^{11B}_{r,0}$ are related to $\delta^{11B}_{r,0}=(\alpha^{11-10}_{r-f})(\delta^{11B}_{f,0}+1000)-1000$, where the equilibrium fractionation factor α^{11-10}_{r-f} of B isotope between rock and fluid is equivalent to $(^{11}B/^{10}B)_r/(^{11}B/^{10}B)_f$. Then, it is combined to Eqn. (6) and the equilibrated isotopic B value of rock ($\delta^{11B}_{r,0}$) can be obtained by,

$$\delta^{11B}_{r,0}=[(\delta^{11B}_0)*C_0*(\alpha^{11-10}_{r-f})-1000*(C_{f,0})*F*(1-(\alpha^{11-10}_{r-f}))]/[(C_{f,0})*F+(\alpha^{11-10}_{r-f})*(C_{r,0})*(1-F)] \qquad (7)$$

$\delta^{11B}_{r,0}$ is received by Eqn. (7) for given δ^{11B}_0 calculated by Eqn. (6). Subsequently,

$\delta^{11B}_{r,0}$ is substituted into Eqn. (6) to calculate a new δ^{11B}_{0} for the next iteration step. The equilibrated isotopic B value of reacted fluid ($\delta^{11B}_{f,0}$) can also be calculated by,

$$\delta^{11B}_{f,0}=[(\delta^{11B}_{0})*C_0-1000*((\alpha^{11\text{-}10}_{r\text{-}f})-1)*(C_{r,0})*(1\text{-}F)]/[(C_{f,0})*F+(\alpha^{11\text{-}10}_{r\text{-}f})*(C_{r,0})*(1\text{-}F) \quad (8)$$

3. Results

Along with our data, we have considered previously published results of hydrothermal vent fluid chemistry, which include: major elements (e.g. Na^+, Cl^-, Mg^{2+}, Ca^{2+}, K^+) and in-situ parameters of pH and temperature of the 2002 and 2003 samples, as well as elemental B and B isotopic composition of 2002 samples (Wu et al., 2011, 2012). The reported results and new analyses of B and B isotopic composition of 2003 samples from Milos are presented in Table 1 and the integrated description of results is presented below. The temperature of the hydrothermal waters recorded during field sampling ranged from 78 to 116 °C in 2002 and 63 to 115 °C in 2003. The measured pH values were much lower than the ambient seawater, the lowest of which (1.6–1.8) were detected in the cave fluid samples. The cave fluid samples are characterized by extremely low pH (pH < 1.9) and low Cl (< 130 mM), B (< 0.6 mM), Mg (< 3mM), as well as other major elements (see Table 1) (Wu et al., 2011; 2012). The high sulfate concentration in Cave #1 and #2 samples (similar as the seawater value) was shown in 2002 and 2003 cave waters (Table 1). Relative to seawater, these waters display a 10% Cl concentration, although near seawater B content with much lighter $\delta^{11}B$ (3.6–7.2‰) (Table 1). In addition, some of the submarine fluid samples with lower than ambient chlorinity seawater (e.g., 02ML-6, 16, 17, 19, 20, 25, 26 and 03ML-22, 26, 34, 41) show characteristic B isotope compositions (27.8–40.1‰) and slightly low B content relative to seawater. Excluding the cave fluid samples, all vent waters show a wide range of B and other major elements, ranging from rather lower to much higher values than seawater. The high-Cl fluid samples are

enriched in Cl and B with maximum concentrations of ~2000 mM and ~6 mM, respectively. These waters have varied B isotopic compositions and the lightest $\delta^{11}B$ 2.1‰ is recorded at D site (03ML-27) in 2003 (Table 1). Note that some fluid samples (e.g., 02ML-14, 15, 18 and 03ML-8, 18, 21, 25, 29, 39) display rather low $\delta^{11}B$ (8.5–24.4‰) and high B content (0.7-2 mM) compared with seawater, but show high Mg content (43-55 mM) relative to the high-Cl fluid samples (Table 1). The B/Cl in cave fluid samples is three times higher ($2.4–4.7\times10^{-3}$) than the ambient seawater (0.71×10^{-3}). The other vent waters have a wide range of B/Cl, from 0.6×10^{-3} to 4.6×10^{-3} (Table 1).

The calculated end-member (EM) composition in the high chlorinity fluid samples from both 2002 and 2003 sampling expeditions, show a rather similar pattern of high Na (833–1689 mM), Cl (1154–1998 mM), K (128–228 mM), Ca (63–130 mM), B (5.32–9.17 mM), and B/Cl ($3.6–4.7\times10^{-3}$), as well as low $\delta^{11}B$ (2.3–6.3‰). The EM composition in the low-chlorinity fluid samples also show low Na (54–469 mM), Cl (73–583 mM), but varied K (7–64 mM), Ca (1–37 mM), and B (0.24–2.9 mM), as well as high B/Cl ($1.2–5.3\times10^{-3}$) and low $\delta^{11}B$ (1.4–10.3 ‰) (Table 2). It is noticeable that 2003 high-Cl fluid samples present relatively higher B content and chlorinity but low $\delta^{11}B$ than in 2002.

4. Discussion

4.1 Genesis of deep reservoir fluids at Milos

Most of the vent waters collected present a mixture of brine and ambient seawater, as shown by the linear mixing trends of the element concentrations and Mg plots. In contrast, the cave fluid samples show large deviation from the mixing trends (see Table 1; Fig. 2) (Wu et al., 2011, 2012). The calculated chemical compositions in the EM liquids were constrained by the deep brines, which therefore must have contained major elements and B concentrations of 2–3 and 6–11 times higher than seawater (see Table 2) (Wu et al., 2011, 2012). Similar

pre-existing brines were reported from the drilled wells results in the Milos geothermal field and therefore represent compositions of hydrothermal liquids at depth (Dotsika et al., 2009; Fitzsimons et al., 1997; Liakopoulos et al., 1991; Valsami-Jones et al., 2005). These high chlorinity and major ions, as well as enriched B content with low $\delta^{11}B$ were likely sourced from unique deep reservoirs containing meteoric water, seawater and local volcanic or magmatic water (Dotsika et al., 2009; Liakopoulos et al., 1991; Naden et al., 2005; Wu et al., 2011, 2012). The B enrichment seems to be induced by reaction with volcanic basement during seawater percolation, while the EM $\delta^{11}B$ in high-Cl fluid samples (2.3–6.3 ‰) falls within the range of island-arc volcanic rocks, -5.3 to +7.3 ‰ (Barth, 1993; Ishikawa and Nakamura, 1994; Smith et al., 1997). The depleted Cl and B contents and extremely low EM $\delta^{11}B$ (5.0 and 1.4 ‰ in 2002 and 2003, respectively) are detected in cave fluid samples (Table 2). However, their dissolved $\delta^{18}O$ and δD in previously collected samples during several expeditions exclude the possibility of meteoric origin (Valsami-Jones et al., 2005). Their hydrological and chemical conditions also remain nearly unchanged at least four years, supporting a seawater-derived source (Valsami-Jones et al., 2005). The $\delta^{18}O$ and δD in high-Cl hydrothermal waters indicate evidence for similar seawater-derived signature (Price et al., 2013). Previous works did not fully establish the origin of the deep brine reservoir, beyond constraining the sources as derived from a seawater component (Naden et al., 2005; Wu et al., 2011, 2012). Overall, the mechanism of deep reservoir formation at Milos could involve the effects of vapor-brine phase separation, fluid/sediment interaction and magmatic addition, these alternative scenarios require further systematic discussion below.

4.2 Role of vapor-brine phase separation in Milos

Foustoukos and Seyfried (2007) found that conservative behavior of B during vapor-brine equilibria, was reflected by similar slopes of the fitting functions for

homogeneous starting fluids with different B compositions. The phase separation processes establish a linear relationship between B/Cl and Cl with a slope of 1:1. This is due to the strong volatility of the neutral hydroxyl-bearing B species. A similar observation has been made in previous experimental and field datasets where the phase separation predominantly controlled hydrothermal system fluid composition (dashed lines in Fig. 3)(Berndt and Seyfried, 1990; Bischoff and Rosenbauer, 1987; You et al., 1994). In contrast, additional water/rock interaction, hydration/dehydration of sediment/basalt and magmatic degassing may cause B addition and lead to deviations. The B/Cl increases depend on the degree of contribution from sedimentary and/or magmatic fluids (Giggenbach, 1995; You et al., 1994).

It is evident that most data of EM high-Cl fluid samples in Milos, presents a deviation from the linear trend of MOR and phase separation experimental data, implying additional contribution. Moreover, a similar correlation between B/Cl and Cl could be observed in the high-Cl deep well waters from the Nisyros system, which revealed a relatively high B/Cl compared with those of hydrothermal waters from Milos, Santorini and Methana systems, reflecting a trend of enhanced degree of contribution from sedimentary and/or magmatic input from west to east along the Aegean volcanic arc (see Fig. 3) (Dotsika et al., 2009, 2010; Kavouridis et al., 1999; Minissale et al., 1997; Shimizu et al., 2005). Some EM low-Cl fluid samples in Milos seem to follow a similar linear trend, but with different initial B, and with some scatter (Fig. 3). The distribution of B/Cl in the low-Cl cave fluid samples and the high-Cl fluid samples do not follow the vapor-brine phase separation linear trend in Figure 3, even though these fluids have previously been interpreted as separated vapor and brine phases resulting from sub-critical phase separation (Valsami-Jones et al., 2005; Wu et al., 2011). Two mechanisms are likely: (1) an effect from sub-critical phase separation at deep reaction zone, but with B loss occurring at surface, resulting in lower B/Cl in cave fluid after vapor segregation; and (2) a mineral contribution (clay minerals hydration/dehydration)

significantly affecting B or Cl, whilst constant B/Cl being maintained in the deep reservoir. Together with B isotopic data, the former is consistent with available natural and experimental studies showing non-detectable or minimal $\delta^{11}B$ fractionation, but likely B lost from a vapor phase in an open system (Palmer and Sturchio, 1990; Liebscher et al., 2005; Spivack et al., 1990). Alternatively, either high Cl fluid or low Cl vapor or even temporary venting of low-Cl fluid, followed by a transition to brine-enriched fluid, is commonly reported in vents (Butterfield and Massoth, 1994; Von Damm and Bischoff, 1987). These observations imply that both low-Cl cave fluid and high-Cl fluid samples with different B/Cl were not separated at the same time in Milos. The correlation of $\delta^{11}B$ and B/Cl seems to indicate that the low-Cl cave and the high-Cl waters are not following the experimental linear trend of phase separation, implying either the loss of B after phase separation or not simultaneous separation of both sets of waters (Fig. 4b). On the other hand, a large degree of hydration/dehydration has not yet been reported due to difficulty in isolation of the effects of phase separation. Moreover, significant $\delta^{11}B$ fractionation should be detectable between the low-Cl cave fluid and high-Cl fluid samples if hydration/dehydration occurs.

4.3 Modeling of end components of reservoir brines

The Milos high-Cl fluid samples with high B and low $\delta^{11}B$ plot close to the vent waters from sediment-hosted hydrothermal system and fumarole condensates from on-land volcanoes (see Fig. 4)(Palmer, 1991; Yamaoka et al., 2015; You et al., 1994). These results imply sediments likely plays an important role in B and B isotopic composition variations in the Milos system; however, other B sources should be taken into consideration (Giggenbach ,1995).

4.3.1 Effect of fluid-rock interaction

Limited B isotope data in volcanic rocks have been reported from the Aegean

volcanic arc, and we used the estimated B in volcanic rocks (B= 100 μg/g, $\delta^{11}B$= -2 ‰) from Leeman et al. (2005) as EM in rocks in the model of fluid-rock interaction (see section 2.3). The distribution coefficient ($D_{r\text{-}f}$) for B was given by experimental data of water interacting with rhyolite at 350°C ($D_{r\text{-}f}$ =1.89, Reyes and Trompetter, 2012). The equilibrium fractionation factor $\alpha^{11\text{-}10}{}_{r\text{-}f}$ between volcanic rock (includes unaltered and altered rhyolite) and fluid was assumed to be 0.985 (at 350°C, Deyhle and Kopf, 2005). The parameters used in the fluid-rock interaction model are summarized in Table 3 and the simulated results in rock and fluid with different iterations and w/r ratios are shown in Figure 5. It is clearly observed that ^{11}B preferentially concentrated in liquids relative to rocks. Rather low B and high $\delta^{11}B$ was calculated in waters after fluid-rock interaction compared to those of Milos EM fluid samples (Fig. 5). In contrast, the B patterns in Milos are similar to the simulated equilibrium curve of fluid-sediment interaction if the calculation involved an EM of modern sediment (B 132 μg/g, $\delta^{11}B$= -6.2 ‰, α=0.987 and $D_{r\text{-}f}$ =2.9 at 350°C); additionally, the calculated values were close to the vent waters from sediment-hosted hydrothermal system (see Fig. 5)(Ishikawa and Nakamura, 1993; Williams et al., 2001; Wunder et al., 2005; Yamaoka et al., 2015; You et al., 1994). Moreover, the Cs and Rb enrichment found in the Milos waters, is also present in sediment-hosted hydrothermal vent waters, sourced from terrigenous sediments containing high illite in oceanic crust; notably, Cs is preferentially partitioned into fluid at ~300°C (Price et al., 2013; Yamaoka et al., 2015; You et al., 1994, 1996). Elevated B, Br, I, NH_4, Cs and Rb in fluid samples have previously been associated with strong fluid-sediment interaction in sediment-hosted systems (e.g., Butterfield et al., 1994; Yamaoka et al., 2015; You et al., 1994). However, there is no geological evidence for any thick sedimentary sequences within the subsurface at Milos. Also, there is a deficiency in organic content within Aegean sediments and biogenic gas fluxes e.g., H_2S, relative to the abiotic fluxes of carbon and sulfur (Fytikas, 1989; Gilhooly et al., 2014; Hodkinson et al.,

1994). The alkalinity in Milos hydrothermal waters ranged from below detection limit to 2.9 mmol/l in 2002 and 2.0 mmol/l in 2003 samples, showing slightly high value compared with the average seawater (~2.4 mmol/l) and vent waters from sediment-starved hydrothermal systems (-0.5-0 mmol/l), but much lower than the waters in sediment-hosted systems (1.9-10.6 mmol/l)(see Table 1)(Campbell et al., 1988; Gamo et al., 1991; Von Damm et al., 1985; Von Damm and Bischoff, 1987). Furthermore, the high-Cl fluid samples show relative low EM Br/Cl ($< 1.02\times10^{-3}$) compared with seawater and vent waters in sediment-hosted systems (1.54×10^{-3} and $>1.76\times10^{-3}$), as well as I/Cl ($< 0.006\times10^{-3}$) which fall within the range of MOR and BAB, and are much lower than sediment-hosted systems ($0.073–0.197\times10^{-3}$)(Price et al., 2013; Wu et al., 2012; You et al., 1994). This conflicts with the assumption that the equilibrated B and $\delta^{11}B$ in the high-Cl fluid samples at Milos could have resulted from simply fluid-sediment interaction. We should therefore consider whether vapor-brine phase separation coupled with halite dissolution can be an alternative to induce the high-Cl fluid with low Br/Cl. However, this can not explain the apparent higher partitioning coefficient of B between vapor and brine. The latter requires much larger amount of halite to satisfy the Br/Cl in high-Cl fluid samples and there is no evidence for the presence of halite-bearing evaporitic rocks on Milos (Berndt and Seyfried, 1997; Foustoukos and Seyfried, 2007; Fytikas, 1989; Liakopoulos et al., 1991; Wu et al., 2012; You et al., 1994). An alternative addition of other high B component with low $\delta^{11}B$ and low Br/Cl and I/Cl can not be excluded.

4.3.2 Magmatic fluid contribution and magma genesis

Dotsika et al. (2009) proposed that seawater and arc magmatic water are the two main contributions to the deep thermal water at Milos, with 70% being magmatic water based on stable isotopic data. An extremely high B/Cl in fumarolic condensates from Vulcano Island was also reported, which deviated from the linear trend of phase separation; magmatic water

was proposed as the source (see Fig. 3)(Leeman et al., 2005). It is therefore important to consider whether a magma derived fluid could have contributed to the composition of the reservoir brines in Milos, and induce a high B. Gilhooly et al. (2014) showed a highly uniform sulfur isotopic composition in H_2S of the venting gases and pore waters ($\delta^{34}S_{H2S}$=2.5‰), indicating that the volcanic inputs were buffered to an initial $\delta^{34}S_{H2S}$ 1.7‰ with subsurface anhydrite veins at ~300°C. These sulfur and carbon isotopes are consistent with those in Nisyros Island that are considered to be derived from rhyodacite magma (Gilhooly et al., 2014; Marini et al., 2002). Abundant metallic vein mineralizations distributed around Milos Island have been classified as Kuroko-type, seawater derived, shallow submarine or hybrid volcanogenic massive sulfide types epithermal system (Kilias et al., 2001; Liakopoulos et al., 2001; Marschik et al., 2010; Naden et al., 2005; Vavelidis and Melfos, 1998). Previous studies have revealed that the equilibrated reaction temperatures of fluid inclusions in metal-rich barite from Milos Island ranging from 260 to 340°C and salinity of 2-6 wt% NaCl equivalent, reflecting possible mixing of magmatic-hydrothermal metal-bearing brine and seawater (Vavelidis and Melfos, 1998). A similar high salinity (>4 wt% NaCl equivalent), $\delta^{18}O$ and δD in fluid inclusions from epithermal mineralization and modern geothermal waters were also observed in Milos system (Naden et al., 2003, 2005). This supports also that fluid inclusion may reflect the source of a geothermal fluid. Alfieris et al (2013) revealed that metallic vein mineralization in western Milos was formed in a submarine setting during episodic injection of magmatic volatiles and dilution of the hydrothermal waters. The trace element enrichments of Li, Zn, Rb, Cs, As, W, Bi, Cd and Tl in gas condensates from a subaerial volcano suggest these contents were preferential transported into gas during magma degassing (Vlastélic et al., 2011). The enrichment of gas compatible elements (e.g. Rb, Cs and As) in the hydrothermal fluids of Milos might be explained in a similar way (Price et al., 2013).

It has been suggested that the relatively heavy $\delta^{11}B$ in island arc lavas compared to basalts (e.g. $\delta^{11}B$= -3.6‰ in fresh MORB samples) resulted from transport of ^{11}B-rich liquids released by dehydration of subducted sediments and/or altered oceanic crusts during subduction (e.g., Spivack and Edmond, 1987; Peacock and Hervig, 1999). This is consistent with the EM $\delta^{11}B$ in high-Cl fluid samples measured in Milos in this study (Table 2). The B, B isotopic composition, Br/Cl and I/Cl in the reservoir brine were influenced by addition of deep fluid, considered to be representative of magma source. Furthermore, we hypothesise that the parent magma in Milos formed with addition of the uprising slab-derived fluid with low Br/Cl and I/Cl released from dehydration of subducted altered oceanic crust/sediment, related to serpentinites, during subduction. These Br/Cl and I/Cl ratios decrease due to gradual release of high Br/Cl and I/Cl liquids during deeper subduction (John et al., 2011; Kendrick et al., 2014). John et al. (2012) indicated an interesting result that individual channelized fluid flow events that are short-lived (~200 years), released from a subducting slab and rapidly delivered to the mantle wedge along mobile hydraulic fractures, could be feeding magma formed beneath the volcanic arc. Bernal et al. (2014) suggested that Cl and Br fractionated from basaltic magma with proportional ratio, were transported identically into glasses and hydrothermal waters. Moreover, the Cl/Br/I ratios in melt remain constant from magma reservoir to the surface, indicating differentiation and degassing of magma did not fractionate these halogens from each other, and that instead they were both predominantly controlled by variation of composition in magma (Balcone-Boissard et al., 2010). The parent magma in Milos is associated with dacite-rhyolite formation, showing depletion in Br and low Br/Cl and highly affected by crustal contamination during magma ascent (Balcone-Boissard et al., 2010; Barton et al., 1983; Gilhooly et al., 2014; Marini et al., 2002). A summarized scenario is proposed whereby the slab-derived liquids with elevated B, ^{11}B-rich and gradual decreasing Br/Cl and I/Cl were released and rose from the subducted

altered oceanic crust/sediment slab. Subsequently these ascending liquids were added into parent magma forming below the Aegean volcanic arc and magmatic fluid or volatiles were transported along an extensive network of cracks to the deep reservoir at Milos during degassing (Fig. 6). This process would create a signature of similar $\delta^{11}B$ with island arc lavas but low in Br/Cl and I/Cl, which is consistent with the reservoir brine in the Milos system (see Table 2)(Barth, 1993; Wu et al., 2011; 2012).

Shimizu et al. (2005) observed a variation of noble gas isotopic composition of gases from Aegean geothermal region, including volcanoes along the arc, back-arc area and surrounding areas. It was suggested that relatively high $^3He/^4He$ ratios with $1.3R_A$ to $6.2R_A$ of gas samples from volcanic arc than those of gases from the back-arc and surrounding areas (0.28 R_A to 2.6 R_A and 0.027 R_A to 1.0 R_A, respectively). In addition, the westward decreasing $^3He/^4He$ ratios along the volcanic arc reflected the declining trend of magmatic activity from east (e.g. Nisyros Island) to west (e.g. Methana), as well as from arc to back-arc region (e.g. Ikaria and Lesvos) (Shimizu et al., 2005). Deep well waters from the Nisyros system are high in Cl and B/Cl relative to those of hydrothermal waters from other Aegean arc systems (Fig. 3). The relatively high B/Cl (2.72 and 10.9×10^{-3}) and near seawater value of Br/Cl ($1.31\text{-}1.39\times10^{-3}$) in well and geothermal waters from Nisyros supported consistently that the highest magmatic activity along the arc and the small degree of subducted material contribution in the magma, but the B enrichment is unlikely to have resulted from slab-fluid (Brombach et al., 2003; Kavouridis et al., 1999; Shimizu et al., 2005). The relatively low Br/Cl ratios in high-Cl waters at Milos ($< 1.02\times10^{-3}$) compared with the Methana system ($1.40\text{-}1.56\times10^{-3}$) is likely due to the slab-fluid sourced from deeper depth of subduction and higher degree of magmatic influence relative to the latter (Dotsika et al., 2010; Shimizu et al., 2005; Wu et al., 2012). The relatively low B/Cl (0.77 and 1.06×10^{-3}) in high-Cl waters from Santorini compared with Milos likely resulted from low B concentration of basaltic lavas in

Santorini system (Francalanci et al., 2005; Minissale et al., 1997). For Chios Island, the slightly low Br/Cl in high salinity spring waters relative to seawater likely induced by the mixture of seawater and groundwater, where the less magmatic contribution in the back-arc region was suggested (Dotsika et al., 2006; Shimizu et al., 2005). Further isotopic B data of these systems would be a useful tracer to clarify the origin and evolution of geothermal waters from Aegean geothermal systems. In addition, the similar Li enrichment and light isotopic composition (10.3 mM and δ^7Li= +1.9‰) observed in the EM high-Cl fluid samples of Milos, and δ^7Li is rather light compared with average MORB or mantle (δ^7Li= +3.7‰ and ~ +4‰), close to the upper continental crust (δ^7Li= 0±2‰). This might be attributed to a flux of slab-derived liquids from subducted sediments (Elliott et al., 2006; Lou et al., 2014; Teng et al., 2004; Tomascak et al., 2008). These episodic injections of magmatic fluid/volatiles are also prime candidates in the formation of abundant metallic vein mineralization, ranging from submarine to subaerial environments (e.g., Alfieris et al, 2013; Kilias et al., 2001; Liakopoulos et al., 2001; Marschik et al., 2010; Naden et al., 2005; Vavelidis and Melfos, 1998).

5. Conclusions

It is unique that low-Cl vapor-like and high-Cl fluid samples are co-existent in the Milos system, supporting a scenario involved subcritical phase separation in a deep reservoir brine. Further, the elevated B/Cl and low δ^{11}B (2.3–6.3 ‰) in end-component high-Cl fluid samples are similar to vent waters from sediment-hosted hydrothermal system or fumarole condensates from on-land volcanos. These observations suggest that additional B from sediment or magmatic fluids play an important role in the B and δ^{11}B in the Milos system. In this study, the B, δ^{11}B, B/Cl and literature data of halogens (Br, I) in hydrothermal waters are found to be sensitive tracers for the geochemistry and origin of reservoir liquids, as well as

the role of subducted sediments in volcanic arc magmatism. The connection and transition between submarine and subaerial system in Milos are also successfully constructed. The major observations of this study are:

1. The distribution of B/Cl in low-Cl cave fluid and high-Cl fluid samples at Milos are interpreted as separated vapor and brine phases, respectively, following a vapor-brine phase separation trend. The most likely mechanism is a sub-critical phase separation, but with boron loss occurring at the surface and resulting in lower B/Cl in cave fluid samples relative to theoretical values after vapor segregation. This suggests that low-Cl fluid and high-Cl fluid samples with different B/Cl were not separated at the same time.
2. The simulated interaction of fluid-sediment instead of fluid-volcanic rock satisfies the observations of B and $\delta^{11}B$ in the equilibrated reservoir liquids from Milos. Moreover, high enrichments of Cs and Rb are associated with terrigenous inputs in the Milos hydrothermal waters. However, there are no major subsurface sedimentary sequences in Milos to explain the relatively low Br/Cl and much lower I/Cl shown in the high-Cl fluid samples. We propose a scenario whereby slab-derived liquids with elevated B, ^{11}B-rich and low Br/Cl and I/Cl, were released and rose from the subducted altered oceanic crust/sediment during subduction. Subsequently these ascending liquids were added into parent magma below the Aegean volcanic arc and magmatic fluid and/or volatiles transported along extensive cracks to deep reservoir brines at Milos during degassing. These episodic injections of magmatic fluids highly influenced the formation of abundant metallic vein mineralization of deposits ranging from submarine to subaerial environment at Milos.

Acknowledgments

We would like to thank Dr. C.H. Chung for instrumental analyses at EDSRC and Dr. M. Walia for her suggestions to improve the manuscript. The authors are also thankful for the

comments and suggestions given from Drs. D.I. Foustoukos and T. Pichler on an early version of the manuscript. The helpful comments from editor and three anonymous reviewers have significantly improved the manuscript. This study was supported by NSC and MOE to YCF. Financial support from S.A.R.G of the National and Kapodistrian University of Athens (E.B) and fieldwork support from the National Geographic Society and the Natural Hisotry Museum (E.V-J) are acknowledged.

References

Agostini, S., Doglioni, C., Innocenti, F., Manetti, P., Tonarini, S., 2010. On the geodynamics of the Aegean rift. Tectonophysics 488, 7-21.

Alfieris, D., Voudouris, P., Spry, P.G., 2013. Shallow submarine epithermal Pb-Zn-Cu-Au-Ag-Te mineralization on western Milos Island, Aegean Volcanic Arc, Greece: Mineralogical, geological and geochemical constraints. Ore Geol. Rev. 53, 159-180.

Balcone-Boissard, H., Villemant, B., Boudon, G., 2010. Behavior of halogens during the degassing of felsic magmas. Geochim. Geophys. Geosyst. 11, Q09005, doi:10.1029/2010GC003028.

Banner, J.L., Hanson, G.N., 1990. Calculation of simultaneous isotopic and trace element variations during water-rock interaction with applications to carbonate diagenesis. Geochim. Cosmochim. Acta 54, 3123-3137.

Barth, S., 1993. Boron isotope variations in nature - a synthesis. Geol. Rundsch. 82(4), 640-651.

Barton, M., Salters, V.J.M., Huijsmans, J.P.P., 1983. Sr isotope and trace element evidence for the role of continental crust in calc-alkaline volcanism on Santorini and Milos, Aegean Sea, Greece. Earth Planet. Sci. Lett. 63, 273-291.

Bebout, G.E., Ryan, J.G., Leeman, W.P., 1993. B-Be systematics in subduction-related metamorphic rocks: characterization of the subducted component. Geochim. Cosmochim. Acta 57, 2227-2237.

Bernal, N.F., Gleeson, S.A., Dean, A.S., Liu, X.M., Hoskin, P., 2014. The source of halogens in geothermal fluids from the Taupo Volcanic Zone, North Island, New Zealand. Geochim. Cosmochim. Acta 126, 265-283.

Berndt, M.E., Seyfried, W.E.Jr., 1990. Boron, bromine, and other trace elements as clues

to the fate of chlorine in mid-ocean ridge vent fluids. Geochim. Cosmochim. Acta 54, 2235-2245.

Berndt, M.E., Seyfried, W.E.Jr., 1997. Calibration of Br/Cl fractionation during subcritical phase separation of seawater: possible halite at 9 to 10°N East Pacific Rise. Geochim. Cosmochim. Acta 61, 2849-2854.

Bischoff, J.L., Dickson, F.W., 1975. Seawater-basalt interaction at 200 °C and 500 Bars - Implications for origin of sea-floor heavy-metal deposits and regulation of seawater chemistry. Earth Planet. Sci. Lett. 25, 385-397.

Bischoff, J.L., Rosenbauer, R.J., 1984. The critical point and two-phase boundary of seawater, 200-500 °C. Earth Planet. Sci. Lett. 68, 172-180.

Bischoff, J.L., Rosenbauer, R.J., 1987. Phase separation in seafloor geothermal systems: An experimental study of the effects on metal transport. Am. J. Sci. 287, 953-978.

Botz, R., Stiiben, D., Winckler, G., Bayer, R., Schmitt, M., Faber, E., 1996. Hydrothermal gases offshore Milos Island, Greece. Chem. Geol. 130, 161-173.

Brombach, T., Caliro, S., Chiodini, G., Fiebig, J., Hunziker, J.C., Raco, B., 2003. Geochemical evidence for mixing of magmatic fluids with seawater, Nisyros hydrothermal system, Greece. Bull. Volcanol. 65, 505-516.

Butterfield, D.A., Massoth, G.J., 1994. Geochemistry of North Cleft segment vent fluids: tempral changes in chlorinity and their possible relation to recent volcanism. J. Geophys. Res. 99, 4951-4968.

Butterfield, D.A., Massoth, G.J., Mcduff, R.E., Lupton, J.E., Lilley, M.D., 1990. Geochemistry of hydrothermal fluids from Axial Seamount hydrothermal emissions study vent field, Juan de Fuca Ridge - Subseafloor boiling and subsequent fluid-rock interaction. J. Geophys. Res. 95, 12895-12921.

Butterfield, D.A., Mcduff, R.E., Franklin, J., Wheat, C.G., 1994. Geochemistry of

hydrothermal vent fluids from Middle valley, Juan de Fuca Ridge. Proc. ODP Sci. Results 139, 395-410.

Campbell, A.C., Palmer, M.R., Klinkhammer, G.P., Bowers, T.S., Edmond, J.M., Lawrence, J.R., Casey, J.F., Thompson, G., Humphris, S., Rona, P., Karson, J.A., 1988. Chemistry of hot springs on the Mid-Atlantic Ridge. Nature 335, 514–519

Campbell, A.C., Edmond, J.M., 1989. Halide systematics of submarine hydrothermal vents. Nature 342, 168-170.

Capaccioni, B., Tassi, F., Vaselli, O., Tadesco, D., Poreda, R., 2007. Submarine gas burst at Panarea Island (southern Italy) on 3 November 2002: A magmatic versus hydrothermal episode, J. Geophys. Res. 112, B05201, doi:10.1029/2006JB004359.

Capaccioni, B., Tassi, F., Vaselli, O., Tadesco, D., Rossi, P.L., 2005. The November 2002 degassing event at Panarea Island (Italy): five months of geochemical monitoring. Ann. Geophys. 48, 755-765.

Dando, P.R., Hughes, J.A., Leahy, Y., Niven, S.J., Taylor, L.J., Smith, C., 1995. Gas venting rates from submarine hydrothermal areas around the Island of Milos, Hellenic Volcanic Arc. Cont. Shelf Res. 15, 913-929.

Deyhle, A., Kopf, A.J., 2005. The use and usefulness of boron isotopes in natural silicate-water systems. Physics and Chemistry of the Earth 30, 1038-1046.

Dotsika, E., Leontiadis, I., Poutoukis, D., Cioni, R., Raco, B., 2006. Fluid geochemistry of the Chios geothermal area, Chios Island, Greece. J. Volcanol. Geotherm. Res. 154, 237-250.

Dotsika, E., Poutoukis, D., Michelot, J.L., Raco, B., 2009. Nature tracers for identifying the origin of the thermal fluids emerging along the Aegean Volcanic arc (Greece): Evidence of Arc-Type Magmatic Water (ATMW) participation. J. Volcanol. Geotherm. Res. 179, 19-32.

Dotsika, E., Poutoukis, D., Raco, B., 2010. Fluid geochemistry of the Methana Peninsula and Loutraki geothermal area, Greece. J. Geochem. Explor. 104, 97-104.

Elliott, T., Thomas, A., Jeffcoate, A., Niu, Y., 2006. Lithium isotope evidence for subduction-enriched mantle in the source of mid-ocean-ridge basalts. Nature 443, 565-568.

Fitzsimons, M.F., Dando, P.R., Hughes, J.A., Thiermann, F., Akoumianaki, I., Pratt, S.M., 1997. Submarine hydrothermal brine seeps off Milos, Greece: Observations and geochemistry. Mar. Chem. 57, 325-340.

Fouquet, Y., Stackelberg, U.V., Charlou, J.L., Donval, J.P., Erzinger, J., Foucher, J.P., Herzig, P., Muhe, R., Soakai, S., Wiedicke, M., Whitechurch, H., 1991. Hydrothermal activity and metallogenesis in the Lau back-arc basin. Nature 349, 778–781.

Foustoukos, D.I., Seyfried, W.E.Jr., 2007. Trace element partitioning between vapor, brine and halite under extreme phase separation conditions. Geochim. Cosmochim. Acta 71, 2056-2071.

Francalanci, L., Vougioukalakis, G.E, Perini, G., Manetti, P., 2005. A West-East traverse along the magmatism of the South Aegean volcanic arc in the light of volcanological, chemical and isotope data. In: Fytikas, M., Vougioulakakis, G. (Eds.), The South Aegean Volcanic Arc: Present Knowledge and Future Perspectives: Elsevier Book Special Series, Developments in Volcanology 7, 65-111.

Fytikas, M., 1989. Updating of the geological and geothermal research on Milos Island. Geothermics 18, 485–496.

Fytikas, M., Innocenti, F., Kolios, N., Manetti, P., Mazzuoli, R., Poli, G., Rita, F., Villari, L., 1986. Volcanology and petrology of volcanic products from the island of Milos and neighbouring islets. J. Volcanol. Geotherm. Res. 28, 297-317.

Gaillardet, J., Lemarchand, D., Gopel, C., Manhes, G., 2001. Evaporation and

sublimation of boric acid: Application for boron purification from organic rich solutions. Geostand. Geoanal. Res. 25(1), 67-75.

Gamo, T., Sakai, H., Kim, E.S., Shitashima, K., Ishibashi, J., 1991. High alkalinity due to sulfate reduction in the CLAM hydrothermal field, Okinawa Trough. Earth Planet. Sci. Lett. 107, 328-338.

Giggenbach, W.F., 1995. Variations in the chemical and isotopic composition of fluids discharged over the Taupo Volcanic Zone. J. Volcanol. Geotherm. Res. 68, 89–116.

Gilhooly, W.P., Fike, D.A., Druschel, G.K., Kafantaris, F.A., Price, R.E., Amend, J.P., 2014. Sulfur and oxygen isotope insights into sulfur cycling in shallow-sea hydrothermal vents, Milos, Greece. Geochem. Trans. 15:12, doi:10.1186/s12932-014-0012-y.

Hershey, J.P., Fernandez, M., Milne, P.J., Millero, F.J., 1986. The ionization of boric acid in NaCl, Na-Ca-Cl and Na-Mg-Cl solutions at 25°C. Geochim. Cosmochim. Acta 50(1), 143-148.

Hinkley, T.K., Tatsumoto, M., 1987. Metals and isotopes in Juan de Fuca Ridge hydrothermal fluids and their associated solid materials. J. Geophys. Res. 92, 11400-11410.

Hodkinson, R.A., Cronan, D.S., Varnavas, S., Perissoratis, C., 1994. Regional geochemistry of sediments from the Hellenic Volcanic Arc in regard to submarine hydrothermal activity. Mar. Georesources Geotechnol. 12, 83-129.

Ishibashi, J., Nakaseama, M., Seguchi, M., Yamashita, T., Doi, S., Sakamoto, T., Shimada, K., Shimada, N., Noguchi, T., Oomori, T., Kusakabe, M., Yamanaka, T., 2008. Marine shallow-water hydrothermal activity and mineralization at the Wakamiko crater in Kagoshima bay, south Kyushu, Japan. J. Volcanol. Geotherm. Res. 173, 84-98.

Ishikawa, T., Nakamura, E., 1993. Boron isotope systematics of marine sediments. Earth Planet. Sci. Lett. 117, 567-580.

Ishikawa, T., Nakamura, E., 1994. Origin of the slab component in arc lavas from across-arc

variation of B and Pb isotopes. Nature 370, 205-208.

John, T., Gussone, N., Podladchikov, Y.Y., Bebout, G.E., Dohmen, R., Halama, R., Klemd, R., Magna, T., Seitz, H., 2012. Volcanic arcs fed by rapid pulsed fluid flow through subducting slabs. Nature Geoscience 5, doi: 10.1038/ngeo1482.

John, T., Scambelluri, M., Frische, M., Barnes, J.D., Bach, W., 2011. Dehydration of subducting serpentinite: Implications for halogen mobility in subduction zones an the deep halogen cycle. Earth Planet. Sci. Lett. 308, 65-76.

Kakihana, H., Kotaka, M., Satoh, S., Nomura, M., Okamoto, M., 1977. Fundamental studies on the ion-exchange separation of boron isotopes. Bull. Chem. Soc. Jpn., 50(1), 158-163, doi: 10.1246/bcsj.50.158.

Kavouridis, T., Kuris, D., Leonis, C., Liberopoulou, V., Leontiadis, J., Panichi, C., La Ruffa, G., Caprai, A., 1999. Isotope and chemical studies for a geothermal assessment of the island of Nisyros (Greece). Geothermics 28, 219-239.

Kendrick, M.A., Arculus, R.J., Danyushevsky, L.V., Kamenetsky, V.S., Woodhead, J.D., Honda, M., 2014. Subduction-related halogens (Cl, Br and I) and H_2O in magmatic glasses from Southwest Pacific Backarc Basins. Earth Planet. Sci. Lett. 400, 165-176.

Kilias, S.P., Naden, J., Cheliotis, I., Shepherd, T.J., Constandinidou, H., Crossing, J., Simos, I., 2001. Epithermal gold mineralisation in the active Aegean Volcanic Arc: the Profitis Ilias deposit, Milos Island, Greece. Miner. Deposita 36, 32-44.

Kilias, S.P., Nomikou, P., Papanikolaou, D., Polymenakou, P.N., Godelitsas, A., Argyraki, A., Carey, S., Gamaletsos, P., Mertzimekis, T.J., Stathopoulou, E., Goettlicher, J., Steininger, R., Betzelou, K., Livanos, I., Christakis, C., Bell, K.C., Scoullos, M., 2013. New insights into hydrothermal vent processes in the unique shallow-submarine arc-volcano, Kolumbo (Santorini), Greece. Scientific Reports 3:2421, doi:10.1038/srep02421.

Klochko, K., Kaufman, A.J., Yao, W., Byrne, R.H., Tossell, J.A., 2006. Experimental

measurement of boron isotope fractionation in seawater. Earth Planet. Sci. Lett. 248, 276-285.

Koschinsky, A., Garbe-Schönberg, D., Sander, S., Schmidt, K., Gennerich, H., Strauss, H., 2008. Hydrothermal venting at pressure-temperature conditions above the critical point of seawater, 5°S on the Mid-Atlantic Ridge. Geology 36, 615-618.

Leeman, W.P., Tonarini, S., Pennisi, M., Ferrara, G., 2005. Boron isotopic variations in fumarolic condensates and thermal waters from Vulcano Island, Italy: Implications for evolution of volcanic fluids. Geochim. Cosmochim. Acta 69(1), 143-163.

Leeman, W.P., Vocke, R.D., McKibben, M.A., 1992. Boron isotopic fractionation between coexiting vapor and liquid in natural geothermal systems. 7th international Symposium on Water-Rock Interaction WRI-7, Park City, Utah, USA, 13-18 July 1992, (eds) YK Kharaka and AS Maest, Rotterdam (AA Balkema) 2, 1007-1010.

Liakopoulos, A., Glasby, G.P., Papavassiliou, C.T., Boulegue, J., 2001. Nature and origin of the Vani manganese deposit, Milos, Greece: an overview. Ore Geol. Rev. 18, 181-209.

Liakopoulos, A., Katerinopoulos, A., Markopoulos, T., Boulegue, J., 1991. A mineralogical petrographic and geochemical study of samples from wells in the geothermal field of Milos Island (Greece). Geothermics 20, 237-256.

Liebscher, A., Meixner, A., Romer, R.L., Heinrich, W., 2005. Liquid-vapor fractionation of boron and boron isotopes: experimental calibration at 400°C/23 MPa to 450°C/42 MPa. Geochim. Cosmochim. Acta 69(24), 5693-5704.

Lonsdale, P.F., 1977. Deep-tow observations at the Mounds abyssal hydrothermal field, Galapagos rift. Earth Planet. Sci. Lett. 36, 92–110.

Lou, U.L., You, C.F., Wu, S.F., Chung, C.H., 2014. Lithium isotope as a proxy for water/rock interaction between hydrothermal fluids and oceanic crust at Milos, Greece. Geophys. Res. Abstr. EGU2014-16-7012, EGU General Assembly 2014, Vienna, Austria.

Marini, L., Gambardella, B., Principe, C., Arias, A., Brombach, T., Hunziker, J.C., 2002. Characterization of magmatic sulfur in the Aegean island arc by means of the $\delta^{34}S$ values of fumarolic H_2S, elemental S, and hydrothermal gypsum from Nisyros and Milos islands. Earth Planet. Sci. Lett. 200, 15-31.

Marschik, R., Bauer, T., Hensler, A., Skarpelis, N., Hölzl, S., 2010. Isotope geochemistry of the Pb-Zn-Ba(-Ag-Au) mineralization at Triades-Galana, Milos Island, Greece. Resour. Geol. 60, 335-347.

Martini, M., Piccardi, G., Cellini Legittimo, P., 1980. Geochemical surveillance of active volcanoes: data on the fumaroles of Vulcano (Aeolian Islands, Italy). Bull. Volcanol. 43, 255-263.

Matsuda, J-I., Senoh, K., Maruoka, T., Sato, H., Mitropoulos, P., 1999. K-Ar ages of the Aegean volcanic rocks and their implication for the arc-trench system. Geochem. J. 33, 369-377.

McCarthy, K.T., Pichler, T., Price, R.E., 2005. Geochemistry of Champagne Hot Springs shallow hydrothermal vent field and associated sediments, Dominica, Lesser Antilles. Chem. Geol. 224, 55-68.

McKenzie, D., 1970. Plate tectonics of the Mediterranean region. Nature 226, 239-243.

McKenzie, D., 1972. Active tectonics of the Mediterranean region. Geophys. J. R. Astron. Soc. 30, 109-185.

Millot, R., Hegan, A., Négrel, P., 2012. Geothermal waters from the Taupo Volcanic Zone, New Zealand; Li, B and Sr isotopes characterization. Appl. Geochem. 27, 677-688.

Minissale, A., Duchi, V., Kolios, N., Nocenti, M., Verrucchi, C., 1997. Chemical patterns of thermal aquifers in the volcanic islands of the Aegean arc, Greece. Geothermics 26, 501-518.

Naden, J., Kilias, S.P., Leng, M.J., Cheliotis, I., Shepherd, T.J., 2003. Do fluid inclusion

preserve $\delta^{18}O$ values of hydrothermal fluids in epithermal systems over geological time? Evidence from paleo- and modern geothermal systems, Milos island, Aegean Sea. Chem. Geol. 197, 143-159.

Naden, J., Kilias, S.P., Darbyshire, D.P.F., 2005. Active geothermal systems with entrained seawater as modern analogs for transitional volcanic-hosted massive sulfide and continental magmato-hydrothermal mineralization: The example of Milos Island, Greece. Geology 33, 541-544.

Palmer, M.R., 1991. Boron isotope systematics of hydrothermal fluids and tourmalines: A synthesis. Chem. Geol. 94, 111-121.

Palmer, M.R., Sturchio, N.C., 1990. The boron isotope systematics of the Yellowstone National Park (Wyoming) hydrothermal system: a reconnaissance. Geochim. Cosmochim. Acta 54, 2811-2815.

Papazachos, C.B., Hatzidimitriou, P.M., Panagiotopoulos, D.G., Tsokas, G.N., 1995. Tomography of the crust and upper mantle in southeast Europe. J. Geophys. Res. 100, 12405-12422.

Peacock, S.M., Hervig, R.L., 1999. Boron isotopic composition of subduction-zone metamorphic rocks. Chem. Geol. 348, 15-26.

Pichler, T., Veizer, J., Hall, G.E.M., 1999. The chemical composition of shallow-water hydrothermal fluids in Tutum Bay, Ambitle Island, Papua New Guinea and their effect on ambient seawater. Mar. Chem. 64, 229-252.

Price, R.E., Savov, I., Planer-Friedrich, B., Bühring, S.I., Amend, J., Pichler, T., 2013. Processes influencing extreme As enrichment in shallow-sea hydrothermal fluids of Milos Island, Greece. Chem. Geol. 348, 15-26.

Prol-Ledesma, R.M., Canet, C., Torres-Vera, M.A., Forrest, M.J., Armienta, M.A., 2004. Vent fluid chemistry in Bahía Concepción coastal submarine hydrothermal system, Baja

California Sur, Mexico. J. Volcanol. Geotherm. Res. 137, 311-328.

Reyes, A.G., Trompetter, W.J., 2012. Hydrothermal water-rock interaction and the redistribution of Li, B and Cl in the Taupo Volcanic Zone, New Zealand. Chem. Geol. 314-317, 96-112.

Ring, U., Glodny, J., Will, T., Thomson, S., 2010. The Hellenic Subduction System: high-pressure metamorphism, exhumation, normal faulting, and large-scale extension. Annu. Rev. Earth Planet. Sci. 38, 45-76.

Ruzié, L., Moreira, M., Crispi, O., 2012. Noble gas isotopes in hydrothermal volcanic fluids of La Soufrière volcano, Guadeloupe, Lesser Antilles arc. Chem. Geol. 304-305, 158-165.

Sedwick, P., Stüben, D., 1996. Chemistry of shallow submarine warm springs in an arc-volcanic setting: Vulcano Island, Aeolian Archipelago, Italy. Mar. Chem. 53(1-2), 147-161.

Seyfried, Jr.W.E., 1987. Experimental and theoretical constraints on hydrothermal alteration processes at Mid-Ocean Ridges. Annu. Rev. Earth Planet. Sci. 15, 317-335.

Seyfried, Jr.W.E., Bischoff, J.L., 1979. Low temperature basalt alteration by seawater: an experimental study at 70 °C and 150 °C. Geochim. Cosmochim. Acta 43, 1937-1947.

Seyfried, Jr.W.E., Janecky, D.R., Mottl, M.J., 1984. Alteration of the oceanic crust: Implications for geochemical cycles of lithium and boron. Geochim. Cosmochim. Acta 48, 557-569.

Seyfried, Jr.W.E., Seewald, J.S., Berndt, M.E., Ding, K., Foustoukos, D.I., 2003. Chemistry of hydrothermal vent fluids from the Main Endeavour Field, Northern Juan de Fuca Ridge: geochemical controls in the aftermath of June 1999 seismic events. J. Geophys. Res. 108, 2429-2452.

Shimizu, A., Sumino, H., Nagao, K., Notsu, K., Mitropoulos, P., 2005. Variation in noble gas

isotopic composition of gas samples from the Aegean arc, Greece. J. Volcanol. Geotherm. Res. 140, 321-339.

Smith, H.J., Leeman, W.P., Davidson, J., Spivack, A.J., 1997. The B isotopic composition of arc lavas from Martinique, Lesser Antilles. Earth Planet. Sci. Lett. 146, 303-314.

Somoza, L., Martínez-Frías, J., Smellie, J.L., Rey, J., Maestro, A., 2004. Evidence for hydrothermal venting and sediment volcanism discharged after recent short-lived volcanic eruptions at Deception Island, Bransfield Strait, Antarctica. Mar. Geol. 203, 119-140.

Spivack, A.J., Edmond, J.M., 1987. Boron isotope exchange between seawater and the oceanic crust. Geochim. Cosmochim. Acta 51, 1033-1043.

Spivack, A.J., Berndt, M.E., Seyfried, W.E., 1990. Boron isotope fractionation during supercritical phase separation. Geochim. Cosmochim. Acta 54, 2337-2339.

Spivack, A.J., Palmer, M.R., Edmond, J.M., 1987. The sedimentary cycle of the boron isotopes. Geochim. Cosmochim. Acta 51, 1939-1949.

Tomascak, P.B., Langmuir, C.H., le Roux, P.J., Shirey, S.B., 2008. Lithium isotopes in global mid-ocean ridge basalts. Geochim. Cosmochim. Acta 72, 1626-1637.

Tassi, F., Capaccioni, B., Caramanna, G., Cinti, D., Montegrossi, G., Pizzino, L., Quattrocchi, F., Vaselli, O., 2009. Low-pH waters discharging from submarine vents at Panarea Island (Aeolian islands, southern Italy) after the 2002 gas blast: Origin of hydrothermal fluids and implications for volcanic surveillance. Appl. Geochem. 24, 246-254.

Urabe, T., Baker, E.T., Ishibashi, J., Feely, R.A., Marumo, K., Massoth, G.J., Maruyama, A., Shitashima, K., Okamura, K., Lupton, J.E., Sonoda, A., Yamazaki, T., Aoki, M., Gendron, J., Greene, R., Kaiho, Y., Kisimoto, K., Lebon, G., Matsumoto, T., Nakamura, K., Nishizawa, A., Okano, O., Paradis, G., Roe, K., Shibata, T., Tennant, D., Vance, T.,

Walker, S.L., Yabuki, T., Ytow, N., 1995. The effect of magmatic activity on hydrothermal venting along the superfast-spreading East pacific rise. Science 269, 1092-1095.

Valsami-Jones, E., Baltatzis, E., Bailey, E.H., Boyce, A.J., Alexander, J.L., Magganas, A., Anderson, L., Waldron, S., Ragnarsdottir, K.V., 2005. The geochemistry of fluids from an active shallow submarine hydrothermal system: Milos island, Hellenic Volcanic Arc. J. Volcanol. Geotherm. Res. 148, 130-151.

Varnavas, S.P., Cronan, D.S., 2005. Submarine hydrothermal activity off Santorini and Milos in the Central Hellenic Volcanic Arc: A synthesis. Chem. Geol. 224, 40-54.

Vavelidis, M., Melfos, V., 1998. Fluid inclusion evidence for the origin of the barite-silver-gold-bearing Pb-Zn mineralization of the Triades area, Milos Island, Greece. Bull. Geol. Soc. Greece 32, 137-144.

Vlastélic, I., Staudacher, T., Bachèlery, P., Télouk, P., Neuville, D., Benbakkar, M., 2011. Lithium isotope fractionation during magma degassing: Constraints from silicic differentiates and natural gas condensates from Piton de la Fournaise volcano (Réunion Island). Chem. Geol. 284, 26-34.

Von Damm, K.L., Edmond, J.M., Measures, C.I., Grant, B., 1985a. Chemistry of submarine hydrothermal solutions at Guaymas Basin, Gulf of California. Geochim. Cosmochim. Acta 49, 2221–2237.

Von Damm, K.L., Edmond, J.M., Grant, B., Measures, C.I., Walden, B., Weiss, R.F., 1985b. Submarine hydrothermal solutions at 21°N, East Pacific Rise. Geochim. Cosmochim. Acta 49, 2197–2220.

Von Damm, K.L., 2000. Chemistry of hydrothermal vent fluids from 9-10°N, East Pacific Rise: “Time zero,” the immediate posteruptive period. J. Geophys. Res. 105,

11203-11222.

Von Damm, K.L., Bischoff, J.L., 1987. Chemistry of hydrothermal solutions from the southern Juan de Fuca Ridge. J. Geophys. Res. 92, 11334-11346.

Von Damm, K.L., Lilley, M.D., Shanks III, W.C., Brockington, M., Bray, A.M., O'Grady, K.M., Olson, E., Graham, A., Proskurowski, G., the SouEPR Science Party, 2003. Extraordinary phase separation and segregation in vent fluids from the southern East Pacific Rise. Earth Planet. Sci. Lett. 206, 365-378.

Wang, B.S., You, C.F., Huang, K.F., Wu, S.F., Chung, C.H., Aggarwal, S.K., Lin, P.Y., 2010. Direct separation of boron from Na- and Ca-rich matrices by sublimation for high precision isotopic measurements on MC-ICP-MS. Talanta 82(4), 1378-1384.

Williams, L.B., Hervig, R.L., Holloway, J.R., Hutcheon, I., 2001. Boron isotope geochemistry during diagenesis: Part I. Experimental determination of fractionation during illitization of smectite. Geochim. Cosmochim. Acta 65, 1769–1782.

Wunder, B., Meixner, A., Romer, R.L., Wirth, R., Heinrich, W., 2005. The geochemical cycle of boron: Constraints from boron isotope partitioning experiments between mica and fluid. Lithos 84, 206–216.

Wu, S.F., You, C.F., Wang, B.S., Valsami-Jones, E., Baltatzis, E., 2011. Two-cells phase separation in shallow submarine hydrothermal system at Milos Island, Greece: Boron isotopic evidence. Geophys. Res. Lett. 38. doi: 10.1029/2011GL047409.

Wu, S.F., You, C.F., Valsami-Jones, E., Baltatzis, E., Shen, M.L., 2012. Br/Cl and I/Cl systematics in the shallow-water hydrothermal system at Milos Island, Hellenic Arc. Mar. Chem. 140-141, 33-43.

Yamaoka, K., Hong, E., Ishikawa, T., Gamo, T., Kawahata, H., 2015. Boron isotope geochemistry of vent fluids from arc/back-arc seafloor hydrothermal systems in the

western Pacific. Chem. Geol. 392, 9-18.

You, C.F., Spivack, A.J., Smith, J.H., Gieskes, J.M., 1993. Mobilization of boron in convergent margins: Implications for the boron geochemical cycle. Geology 21(3), 207-210.

You, C.F., Butterfield, D.A., Spivack, A.J., Gieskes, J.M., Gamo, T., Campbell, A.J., 1994. Boron and halide systematics in submarine hydrothermal systems - Effects of phase-separation and sedimentary contributions. Earth Planet. Sci. Lett. 123, 227-238.

You, C.F., Castillo, P.R., Gieskes, J.M., Chan, L.H., Spivack, A.J., 1996. Trace element behavior in hydrothermal experiments: implications for fluid processes at shallow depths in subduction zones. Earth Planet. Sci. Lett. 140, 41-52.

Figure captions

Figure 1:

A map of the study area, located within the submarine hydrothermal system of Milos Island, which is situated in the central part of the Aegean Volcanic Arc in the Aegean Sea, Greece. All fluid samples except cave fluid samples were collected in the Palaeohori Bay.

Figure 2:

Plots (a), (b) and (c) are correlations of dissolved Mg concentration and elemental Na, Cl and B in all vent waters collected in 2002 and 2003 (The Na, Cl concentration data from two separate expeditions and B data from 2002; all data are from Wu et al. (2011; 2012)). Mg is a reactive component in hydrothermal systems and used to calculate chemical compositions of end-member vent fluid at each sites by extrapolating the correlation of Mg concentration with other dissolved ions and assuming Mg=0 in the pure hydrothermal fluid. (d) Plot of chlorinity and B/Cl ratio in all hydrothermal waters. The high chlorinity fluid samples display a mixing trend between seawater and high-Cl waters. (e) Plot of chlorinity and B isotopic composition for all vent waters. $\delta^{11}B$ and Cl content show a negative correlation with two significant end-member waters: seawater and a high-Cl fluid with high-$\delta^{11}B$ and low-$\delta^{11}B$, respectively. Cave fluid samples display low-Cl concentration and much lighter $\delta^{11}B$ compared with seawater. (f) Correlation of Mg concentration normalized to B concentration and $\delta^{11}B$ in all vent waters. The end member $\delta^{11}B$ can be defined from this linear correlation by assuming Mg content is zero in pure end-member hydrothermal fluid (Hinkley and Tatsumoto, 1987).

Figure 3:

Plot of end-member Cl and B/Cl ratio (log scale) from all vent waters collected in Milos, as well as hydrothermal, geothermal waters and fumarolic condenses from various geological settings: MOR (Butterfield and Massoth, 1994; Campbell et al., 1988; Koschinsky et al., 2008; Von Damm et al., 2003), BAB and SR (Yamaoka et al., 2015; You et al., 1994), Aegean

geothermal systems (Dotsika et al., 2010; Kavouridis et al., 1999; Minissale et al., 1997) and subaerobic volcanoes (Martini et al., 1980; Millot et al., 2012). The phase separation experimental data is from Spivack et al. (1990). The grey arrow indicates the direction of boron addition.

Figure 4:

Plot of end-member $\delta^{11}B$ and (a) B content and (b) B/Cl ratio in all vent waters collected from Milos, as well as hydrothermal, geothermal waters and fumarolic condensates from various natural systems: MOR (Butterfield and Massoth, 1994; Campbell et al., 1988; Koschinsky et al., 2008; Von Damm et al., 2003), BAB and SR (Yamaoka et al., 2015; You et al., 1994) and subaerial volcanoes (Leeman et al., 2005; Millot et al., 2012). The phase separation experimental data is from Spivack et al. (1990). The inset plot of plot (b) shows the correlation of EM $\delta^{11}B$ and B/Cl ratio in log scale. Most of the EM high-Cl data with high elemental B and low $\delta^{11}B$ from Milos plot far from the MOR data and scatter close to fumarole condensates of on-land volcanoes and vent waters from sediment-hosted hydrothermal system in the Okinawa Trough. The grey arrow indicates that the B addition resulted from varied degee of sedimentary and/or magmatic contribution. The grey dashed arrow represents the supercritical phase separation effect on B/Cl ratio in low-Cl vapor and high-Cl liquid phases.

Figure 5:

Plot of $\delta^{11}B$ and elemental B concentration in end-component waters from Milos, as well as the equilibrium composition of fluid and rock after the fluid-rock/sediment interaction simulation using different end-components including percolated seawater, volcanic rock and modern marine sediment. The black solid and dashed curve lines are the equilibrium curves in the final fluid and rock separately with different fluid-rock ratios during fluid-volcanic rock interaction. In addition, the grey solid curve shows the final equilibrated composition

curve of fluid during fluid-marine sediment interaction. The description and calculation of fluid-rock/sediment interaction are described in more detail in the text.

Figure 6:

Schematic cross section of the Hellenic subduction system, showing the evolution of a deep reservoir under the Milos system (modified from Alfieris et al., 2013, Kilias et al., 2013 and Peacock and Hervig, 1999). The potential origins of chemical constituents in vent waters include seawater, sediment contribution and/or magmatic fluids. We hypothesise a scenario showing that (1) the dehydration of subducted altered oceanic crust/sediment induces the release of high $\delta^{11}B$ and Br/Cl fluid relative to the residue sediment during initial subduction at shallow depth; (2) the slab-derived liquids with elevated B content, relatively light $\delta^{11}B$, gradual decreasing Br/Cl and I/Cl are released from residue subducted altered oceanic crust/sediment at great depth; (3) subsequently, these ascending liquids are added into parent magma forming below the Aegean volcanic arc; and (4) these episodic injections of magmatic fluid and/or volatiles transported along extensive fractures to the deep brine reservoir at Milos during degassing, have a major influence on the formation of abundant metallic vein mineralization and hydrothermal deposits ranging from submarine to subaerial.

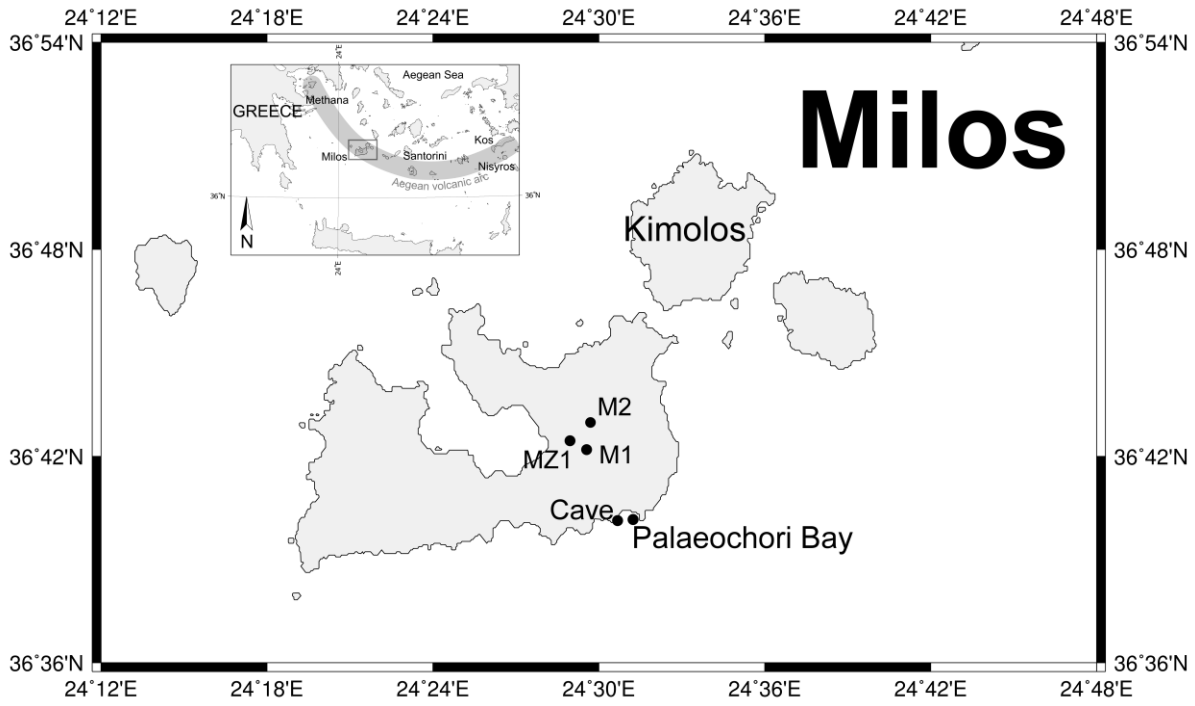

Fig. 1

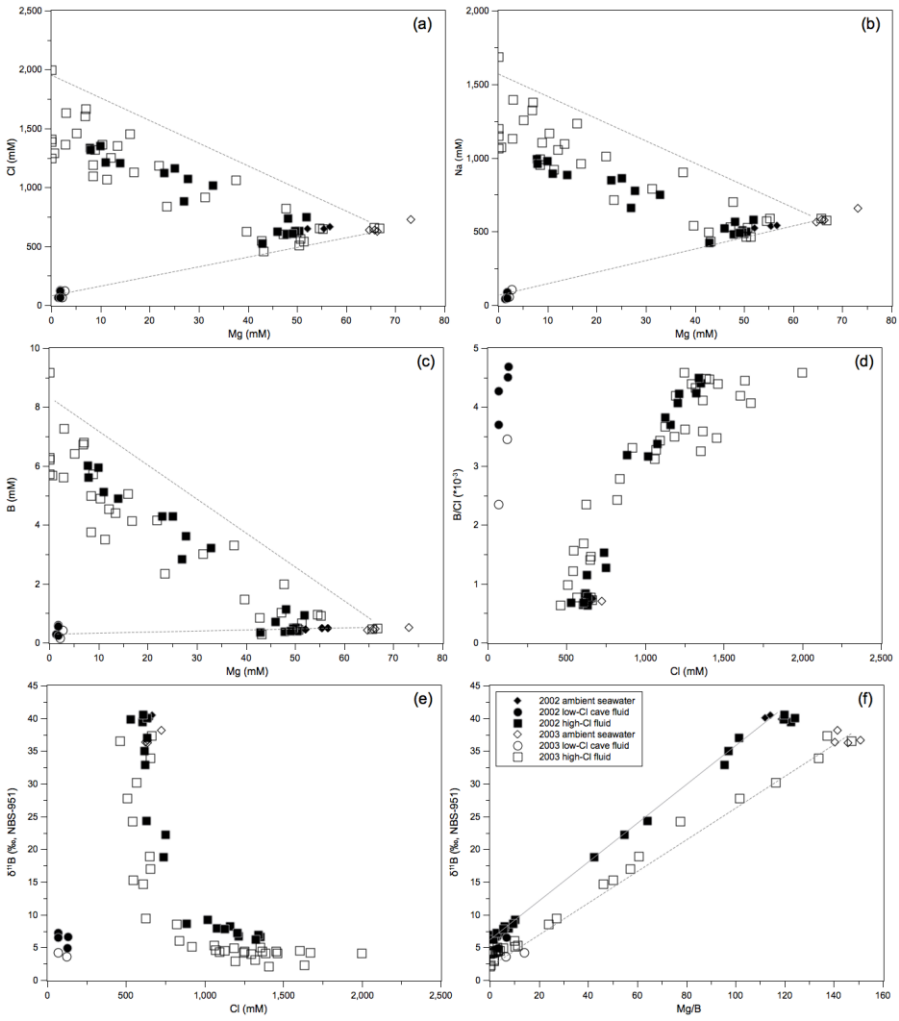

Fig. 2

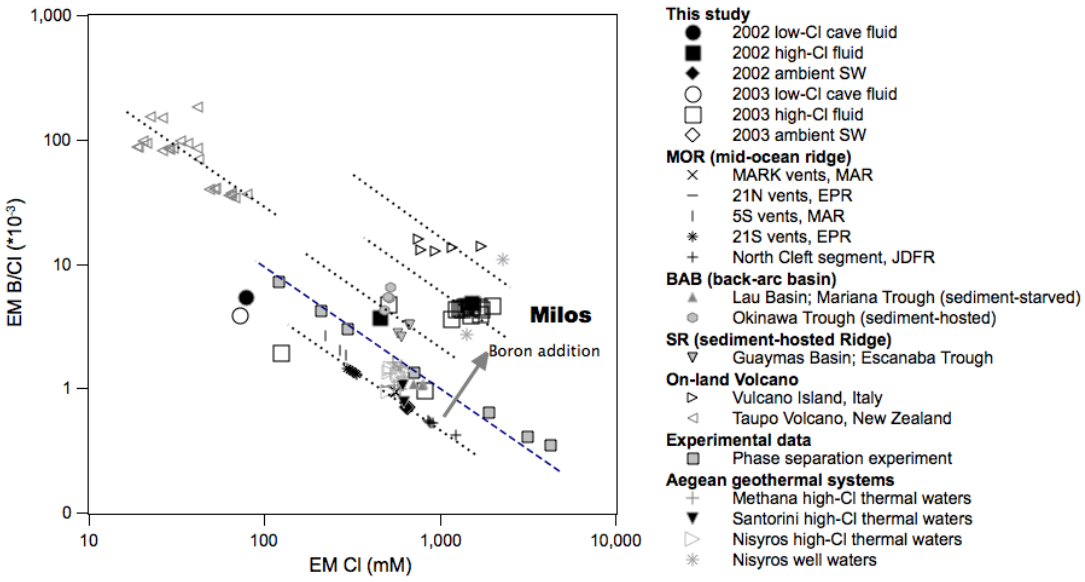

Fig. 3

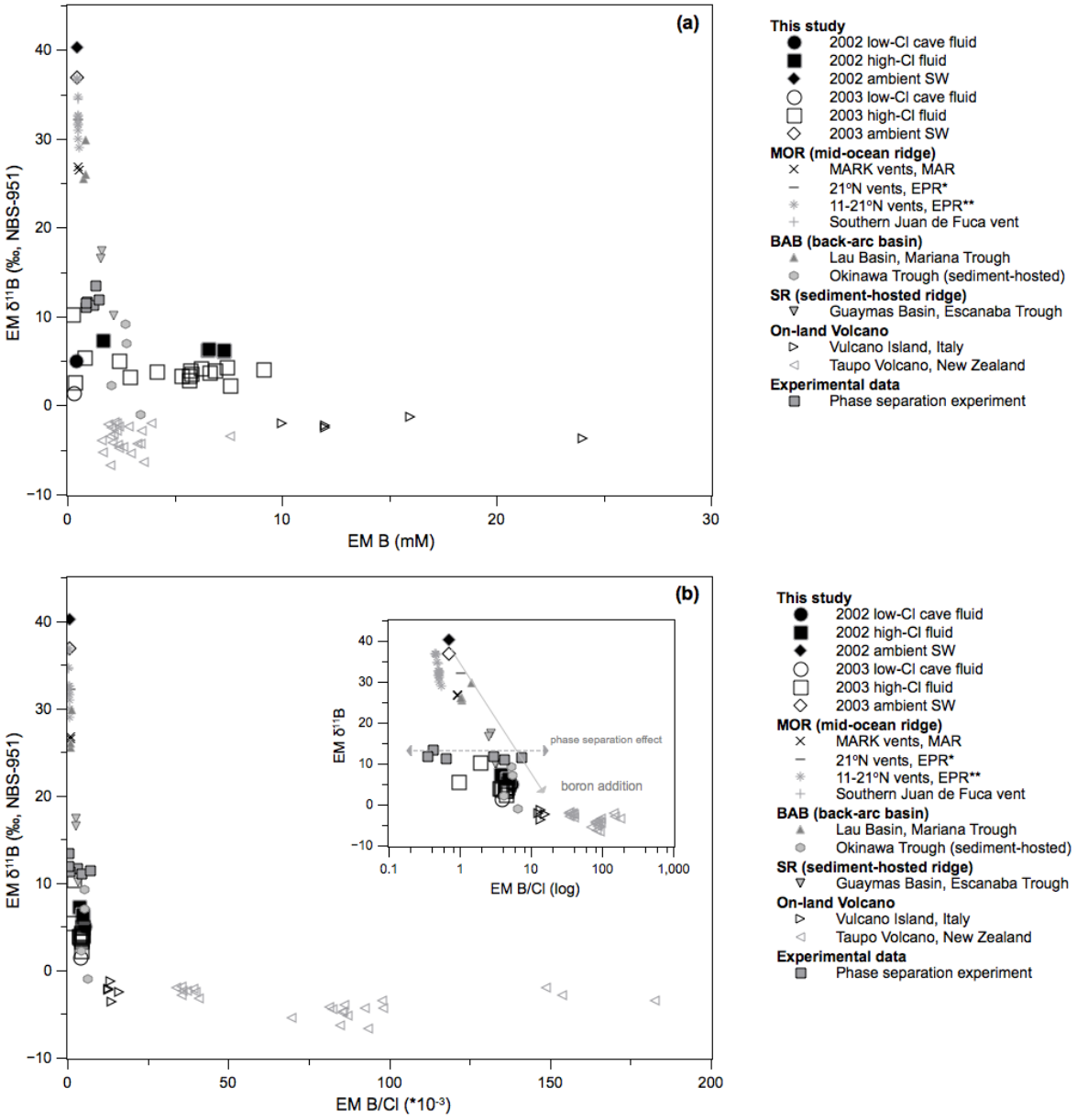

Fig. 4

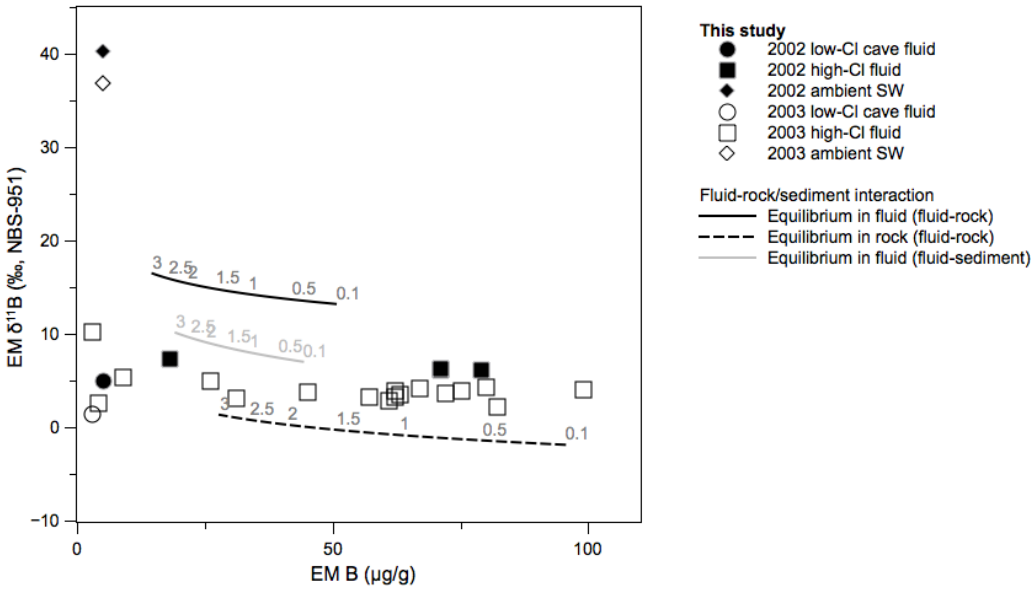

Fig. 5

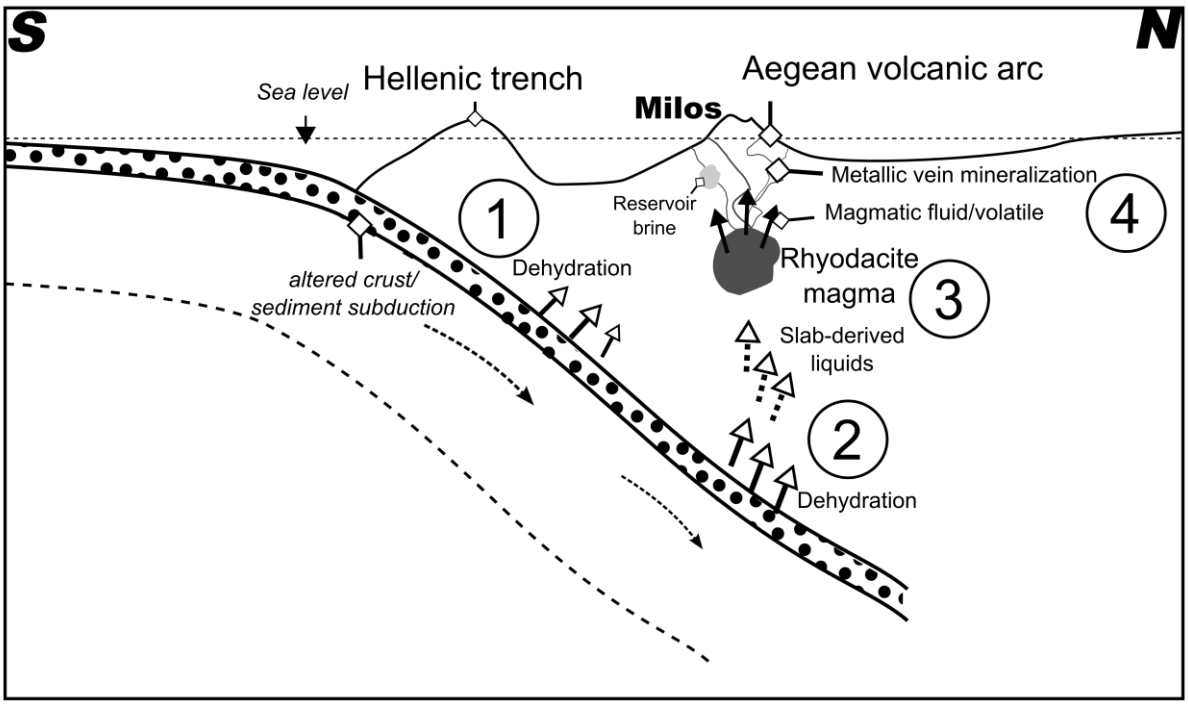

Fig. 6

Table 1. Observed compositions of the hydrothermal vent waters in 2002 and 2003 samples at Milos. The table shows isotopic B composition, concentrations of B, other major elements and dissolved H_2S, as well as the pH, total alkalinity and temperature measured in the hydrothermal waters and local seawater.

Sample no.	Description	Ref.	pH	T (°C)	Alk_t[c] (mmol/l)	H_2S[d] (mM)	Mg (mM)	Na (mM)	Cl (mM)	K (mM)	SO_4[f] (mM)	Ca (mM)	Sr (mM)	B (mM)	$\delta^{11}B$ (‰, NBS 951)	B/Cl ($\times10^{-3}$)
2002 samples		*a*														
02ML-1	seawater		8.08	28.5	2.9	n.a.[e]	55.5	535	648	14	27	11	0.10	0.50	40.08	0.77
02ML-4	cave 1		1.81	91.4	n.a.	0.00	1.8	89	128	13	21	9	0.05	0.60	6.68	4.69
02ML-5	cave 2		1.63	78.2	n.a.	0.02	1.3	45	65	7	27	6	0.02	0.28	7.24	4.27
02ML-6	A1		5.82	110.7	2.2	1.60	50.0	486	614	14	22	11	0.09	0.52	35.05	0.84
02ML-7	seawater		8.03	39.7	2.9	n.a.	56.7	542	665	14	26	12	0.10	0.50	40.48	0.75
02ML-8	B1		6.17	81.3	1.2	0.20	27.7	777	1075	99	12	45	0.33	3.63	7.99	3.38
02ML-9	B2		6.19	98.5	2.6	b.d.[e]	25.1	864	1161	114	11	52	0.38	4.29	8.25	3.70
02ML-10	D1		6.45	86.0	1.4	0.10	32.8	752	1019	88	15	41	0.31	3.22	9.30	3.16
02ML-11	F1		5.45	114.1	0.6	b.d.	22.9	850	1126	117	9	50	0.38	4.30	7.82	3.82
02ML-12	D2		3.43	101.3	b.d.	b.d.	7.8	993	1338	161	6	71	0.52	6.02	6.91	4.50
02ML-13	B2		3.76	98.5	b.d.	b.d.	9.9	979	1352	157	4	69	0.51	5.96	6.62	4.41
02ML	E		6.	88.0	2.2	b.d.	48.	566	73	31	22	18	0.14	1.1	18.85	1.53

-14		02				1		9					3		
02ML-15	E	6.31	88.0	2.3	0.64	51.9	583	748	26	23	16	0.13	0.95	22.20	1.27
02ML-16	F2	6.90	112.3	2.8	0.04	49.6	508	619	16	26	12	0.10	0.52	32.89	0.84
02ML-17	A2	5.35	110.2	2.6	30	47.8	482	605	13	24	10	0.09	0.39	39.51	0.65
02ML-18	A4	5.25	112.4	2.4	32	46.0	525	627	21	22	13	0.11	0.72	24.36	1.15
02ML-19	C1	5.18	115.7	2.6	36	50.4	502	634	13	23	11	0.09	0.41	40.03	0.64
02ML-20	C2	5.23	115.0	2.7	40	42.9	423	528	11	24	9	0.08	0.36	39.85	0.68
02ML-21	seawater	8.00	30.2	2.9	n.a.	52.1	524	648	13	27	11	0.09	0.44	39.89	0.68
02ML-22	D3	3.78	114.1	b.d.	0.10	13.9	887	1207	132	7	60	0.44	4.91	7.22	4.07
02ML-23	D1A	5.75	86.0	1.4	0.65	11.0	893	1214	140	6	60	0.45	5.13	6.77	4.23
02ML-24	D2A	3.29	80.9	b.d.	0.20	7.9	961	1322	151	5	66	0.48	5.61	6.28	4.24
02ML-25	G2A	5.43	111.5	2.6	18	49.6	497	633	14	24	11	0.09	0.49	37.06	0.78
02ML-26	G3	5.67	82.0	2.9	26	49.1	490	607	12	25	10	0.09	0.41	40.55	0.68
02ML-27	D2B	6.08	96.6	1.1	0.05	27.0	660	885	77	16	36	0.27	2.83	8.67	3.19
02ML-28	seawater	8.21	24.5	3.0	b.d.	49.2	501	624	13	27	10	0.09	0.41	40.54	0.66

02ML-29	cave 1		1.74	91.0	n.a.	b.d.	1.8	91	125	13	22	9	0.04	0.56	4.90	4.51
02ML-30	cave 2		1.77	90.0	n.a.	0.1	1.7	49	68	7	26	5	0.02	0.25	6.57	3.70
2003 samples		*b*														
03ML-1	seawater		7.85	31.2	1.6	0.01	65.8	580	635	12	23	13	0.12	0.45	36.27	0.71
03ML-2	GE4		5.47	106.7	1.1	24	65.7	590	660	13	26	13	0.11	0.48	37.32	0.73
03ML-3	D2A		4.27	88.5	0.0	0.2	2.8	1130	1366	147	7	87	0.57	5.62	4.43	4.12
03ML-4	seawater		8.1	31	1.3	b.d.	73.1	656	726	13	29	15	0.12	0.52	38.16	0.71
03ML-5	cave 1		1.64	94.4	0.0	0	2.7	106	121	11	20	9	0.04	0.42	3.64	3.46
03ML-6	cave 2		1.59	81.1	0.0	0.02	2.2	57	67	5	24	5	0.01	0.16	4.21	2.35
03ML-7	D2A		3.3	88.5	b.d.	0.18	12.1	1058	1252	138	6	70	0.53	4.54	4.43	3.62
03ML-8	E		5.82	107.1	1.9	9.2	55.2	589	648	23	20	19	0.14	0.91	18.88	1.41
03ML-9	D1A		3.66	78.3	b.d.	0.7	16.7	962	1128	122	7	63	0.47	4.14	4.48	3.67
03ML-10	D west		4.06	82.7	n.a.	6.4	21.9	1013	1185	122	n.a.	61	0.48	4.15	4.93	3.50
03ML-11	O		5.45	84	0.7	0.3	2.9	1394	1634	178	9	107	0.71	7.28	2.34	4.45
03ML-12	K		4.98	107	0.2	0.85	6.8	1324	1603	164	9	98	0.68	6.73	4.56	4.20
03ML	L4		4.	104.	1.1	0.3	7.0	1379	16	171	7	101	0.69	6.80	4.18	4.07

-13		15	1					69							
03ML-14	L2	4.9	114.2	b.d.	0.3	15.9	1237	1454	161	8	79	0.59	5.06	4.43	3.48
03ML-15	L5	6.63	62.5	1.0	0.3	37.5	904	1060	82	23	52	0.37	3.31	5.30	3.12
03ML-16	P	5.26	68.7	0.5	8.8	5.1	1256	1460	155	10	100	0.64	6.42	4.09	4.40
03ML-17	M	5.47	114.6	0.7	0.15	0.0	1689	1998	228	3	130	0.91	9.17	4.09	4.59
03ML-18	L1	5.77	111.2	1.5	3.4	54.5	573	655	24	28	19	0.15	0.96	17.01	1.46
03ML-19	J	5.66	104.2	0.7	4	39.6	543	626	34	21	23	0.17	1.47	9.46	2.35
03ML-20	L6	4.98	113.8	0.0	0.2	13.4	1098	1351	146	10	67	0.50	4.40	5.06	3.26
03ML-21	N	6.14	112.2	1.5	n.a.	47.7	702	821	47	26	33	0.24	2.00	8.52	2.43
03ML-22	Q	5.82	110.1	1.7	10.8	50.7	526	566	14	21	11	0.09	0.44	30.22	0.77
03ML-23	I	3.33	107.9	0.0	0.15	10.3	1170	1366	159	5	75	0.58	4.91	4.39	3.59
03ML-24	H	3.7	95.7	0.9	2	0.0	1151	1387	157	5	90	0.62	6.23	4.15	4.49
03ML-25	A1	4.6	110.3	0.0	10.4	42.7	495	546	20	17	12	0.11	0.86	15.33	1.57
03ML-26	C1	5.46	110.3	0.9	17	43.2	434	460	10	18	9	0.07	0.29	36.51	0.64
03ML-27	D, diffuse	4.72	71-106.5	0.0	0.26	0.0	1201	1407	156	5	94	0.63	6.29	2.11	4.47
03ML-28	seawater	8.05	29	1.6	n.a.	66.3	577	626	12	23	13	0.11	0.47	36.34	0.75

03ML-29	C1	5.33	110.3	0.5	0.1	51.3	467	542	14	21	12	0.10	0.66	24.28	1.22
03ML-30	A4	5.51	111.9	0.2	0.45	23.5	716	837	80	9	33	0.27	2.34	6.05	2.79
03ML-31	D3	6.42	108.6	0.2	0.02	31.2	790	916	77	20	47	0.33	3.03	5.18	3.31
03ML-32	B1	3.89	81.3	b.d.	0.6	11.3	922	1068	122	6	54	0.41	3.51	4.63	3.28
03ML-33	seawater	7.9	36.9	2.0	n.a.	64.7	564	636	12	26	13	0.11	0.43	36.68	0.67
03ML-34	GE2A	6.2	106.6	2.0	3	66.7	578	652	13	24	14	0.11	0.50	33.92	0.77
03ML-35	B2	3.43	96.8	b.d.	0.26	8.5	954	1095	132	4	57	0.43	3.75	4.34	3.43
03ML-36	F1	3.33	108.1	b.d.	0.04	0.6	1072	1292	139	6	81	0.56	5.68	4.07	4.40
03ML-37	F2	5.2	108	0.0	0.11	8.5	993	1192	123	8	73	0.50	5.00	2.96	4.19
03ML-38	A5	5.03	104.1	0.5	0.14	8.9	1103	1319	138	6	72	0.52	5.72	3.08	4.33
03ML-39	E	6.58	92.2	1.5	0.07	47.2	532	606	25	19	19	0.15	1.03	14.71	1.69
03ML-40	D2C	3.76	90.6	0.0	0.5	0.0	1063	1247	138	6	86	0.56	5.73	4.19	4.59
03ML-41	A4	5.57	111.9	1.0	19	50.4	466	507	12	19	11	0.09	0.50	27.79	0.98

[a] The pH, temperature, Major elements (Na, Cl, Mg, Ca, K), elemental B and $\delta^{11}B$ data of 2002 fluid samples are from Wu et al. (2011).

[b] The pH, temperature, Na, Cl, Mg and K data of 2003 fluid samples are from Wu et al. (2012).

[c] Alk_t, Total Alkalinity

[d] Concentration of dissolved H_2S in fluid

[e] n.a., no analyzed; b.d., below detection

[f] The concentration of SO_4 in vent samples during two expeditions were analyzed by ion chromatography (IC)

Table 2. End-component compositions of the hydrothermal vent waters in 2002 and 2003 samples at Milos. The table shows end-member $\delta^{11}B$, concentrations of B, other major and minor elements in the vent waters from each sampling site. The values were calculated from the measured values based on the vent fluid-seawater mixing trend for Mg, following a linear regression and assuming Mg=0 in the pure hydrothermal fluid. In addition, the end-member $\delta^{11}B$ value was calculated based on the linear correlation of Mg/B and $\delta^{11}B$ (details of the calculation are described in the results section).

Sample no.	Description	Ref.	Na (mM)	Cl (mM)	K (mM)	Ca (mM)	Sr (mM)	B (mM)	$\delta^{11}B$ (‰, NBS 951)	B/Cl ($\times10^{-3}$)
2002 samples		*a*								
02ML-1	seawater									
02ML-4	cave 1		54	79	10	7	0.03	0.42	5.01	5.34
02ML-5	cave 2		54	79	10	7	0.03	0.42	5.01	5.34
02ML-6	A1									
02ML-7	seawater									
02ML-8	B1		1094	1537	193	83	0.61	7.29	6.14	4.74
02ML-9	B2		1094	1537	193	83	0.61	7.29	6.14	4.74
02ML-10	D1		1022	1408	176	76	0.55	6.54	6.19	4.65
02ML-11	F1		1109	1509	197	80	0.61	7.29	6.19	4.83
02ML-12	D2		1022	1408	176	76	0.55	6.54	6.19	4.65
02ML-13	B2		1094	1537	193	83	0.61	7.29	6.14	4.74
02ML-14	E		833	1415	173	69	0.50	6.59	6.34	4.66
02ML-15	E		833	1415	173	69	0.50	6.59	6.34	4.66
02ML-16	F2		1109	1509	197	80	0.61	7.29	6.19	4.83
02ML-17	A2									
02ML-18	A4									
02ML-19	C1									
02ML-20	C2									
02ML-21	seawater									
02ML-22	D3		1022	1408	176	76	0.55	6.54	6.19	4.65
02ML-23	D1A		1022	1408	176	76	0.55	6.54	6.19	4.65
02ML-24	D2A		1022	1408	176	76	0.55	6.54	6.19	4.65
02ML-25	G2A								17.38	

02ML-26	G3								17.38	
02ML-27	D2B		1022	1408	176	76	0.55	6.54	6.19	4.65
02ML-28	seawater									
02ML-29	cave 1		54	79	10	7	0.03	0.42	5.01	5.34
02ML-30	cave 2		54	79	10	7	0.03	0.42	5.01	5.34
2003		*b*								
samples										
03ML-1	seawater									
03ML-2	GE4								5.41	
03ML-3	D2A		1135	1346	153	87	0.60	5.80	3.51	4.30
03ML-4	seawater									
03ML-5	cave 1		62	73	8	7	0.03	0.28	1.44	3.86
03ML-6	cave 2		62	73	8	7	0.03	0.28	1.44	3.86
03ML-7	D2A		1135	1346	153	87	0.60	5.80	3.51	4.30
03ML-8	E		409	507	57	34	0.23	2.40	4.97	4.74
03ML-9	D1A		1135	1346	153	87	0.60	5.80	3.51	4.30
03ML-10	D west		1135	1346	153	87	0.60	5.80	3.51	4.30
03ML-11	O		1430	1677	185	111	0.74	7.58	2.25	4.52
03ML-12	K		1406	1710	181	108	0.74	7.43	4.33	4.35
03ML-13	L4		1391	1689	191	99	0.71	6.63	3.73	3.93
03ML-14	L2		1391	1689	191	99	0.71	6.63	3.73	3.93
03ML-15	L5		1391	1689	191	99	0.71	6.63	3.73	3.93
03ML-16	P		1310	1525	167	107	0.69	6.90	3.91	4.53
03ML-17	M		1689	1998	228	130	0.91	9.17	4.09	4.59
03ML-18	L1		1391	1689	191	99	0.71	6.63	3.73	3.93
03ML-19	J		469	583	64	37		2.90	3.17	4.97
03ML-20	L6		1391	1689	191	99	0.71	6.63	3.73	3.93
03ML-21	N		962	1218	129	82		5.68	2.90	4.67
03ML-22	Q		319	295	17	5		0.34	2.61	1.16
03ML-23	I		1274	1494	186	86	0.66	5.71	3.91	3.82
03ML-24	H		1151	1387	157	90	0.62	6.23	4.15	4.49
03ML-25	A1		1021	1226	139	66	0.50	5.32	3.35	4.34
03ML-26	C1		131	124	7	1	0.01	0.24	10.29	1.92

03ML-27	D, diffuse	1135	1346	153	87	0.60	5.80	3.51	4.30
03ML-28	seawater								
03ML-29	C1	131	124	7	1	0.01	0.24	10.29	1.92
03ML-30	A4	1021	1226	139	66	0.50	5.32	3.35	4.34
03ML-31	D3	1135	1346	153	87	0.60	5.80	3.51	4.30
03ML-32	B1	997	1155	147	63	0.48	4.17	3.86	3.61
03ML-33	seawater								
03ML-34	GE2A							5.41	
03ML-35	B2	997	1155	147	63	0.48	4.17	3.86	3.61
03ML-36	F1	1065	1286	140	82	0.56	5.70	3.31	4.43
03ML-37	F2	1065	1286	140	82	0.56	5.70	3.31	4.43
03ML-38	A5	1021	1226	139	66	0.50	5.32	3.35	4.34
03ML-39	E	409	507	57	34	0.23	2.40	4.97	4.74
03ML-40	D2C	1135	1346	153	87	0.60	5.80	3.51	4.30
03ML-41	A4	1021	1226	139	66	0.50	5.32	3.35	4.34

a The end-component composition of elemental (Na, Cl, Mg, Ca, K and B) and isotopic data ($\delta^{11}B$) in 2002 water samples were calculated by the previously data from Wu et al. (2011).

b The end-component concentration of Na, Cl, Mg and K in 2003 fluid samples were calculated by the previously reported data from Wu et al. (2012).

Table 3. End-member values and parameters used in the fluid-rock/sediment interaction model.

Fluid-rock/sediment interaction	End components	B (ppm)	$\delta^{11}B$ (‰, NBS951)	Isotopic fractionation factor ($\alpha^{11\text{-}10}_{r\text{-}f}$)	Distribution coefficient ($D_{r\text{-}f}$)
Seawater/Volcanic rocks	SW	4.5	39.5	0.985[a]	1.89[a]
	Rocks[b]	100	-2		
Seawater/Marine sediments	SW	4.5	39.5	0.987[c]	2.9[c]
	Sediments[d]	116	-11.7		

[a] Boron isotopic fractionation factor between volcanic rock (unaltered and altered rhyolite) and fluid ($\alpha^{11\text{-}10}_{r\text{-}f}$=0.985) and its distribution coefficient between rhyolite and fluid ($D_{r\text{-}f}$=1.89) from Deyhle and Kopf (2005) and Reyes and Trompetter (2012), respectively.

[b] End-component concentration for B and B isotopic composition of volcanic rocks is from Leeman et al (2005).

[c] Boron isotopic fractionation factor between sediment and fluid ($\alpha^{11\text{-}10}_{r\text{-}f}$=0.987) and its distribution coefficient between sediment and fluid ($D_{r\text{-}f}$=2.9) from Wunder et al (2005) and Yamaoka et al (2015), respectively.

[d] B concentration and isotopic B end-component of marine sediment from Ishikawa and Nakamura (1993).

[e] In this study, a constant porosity in volume fraction (P=20%) was assumed, whereas the densities of the fluid and solid rock (ρ_f=1.0 and ρ_r=2.5 g/cc) used in the fluid-rock/sediment interaction simulation are from Leeman et al (2005).

Research Highlights:

1. High-Cl and low-Cl fluids with high B/Cl and distinct low $\delta^{11}B$ were detected at Milos
2. Sediment/magmatic fluids contributions play important role in vent fluid chemistry
3. B isotopes and Br/I/Cl ratios support slab-derived addition in Milos parent magma
4. Deep water reservoirs were affected by magmatic volatiles via slab-derived processes